

Rank $2r$ iterative least squares: efficient recovery of ill-conditioned low rank matrices from few entries

Jonathan Bauch* Boaz Nadler* Pini Zilber*

January 1, 2022

Abstract

We present a new, simple and computationally efficient iterative method for low rank matrix completion. Our method is inspired by the class of factorization-type iterative algorithms, but substantially differs from them in the way the problem is cast. Precisely, given a target rank r , instead of optimizing on the manifold of rank r matrices, we allow our interim estimated matrix to have a specific over-parametrized rank $2r$ structure. Our algorithm, denoted **R2RILS**, for rank $2r$ iterative least squares, thus has low memory requirements, and at each iteration it solves a computationally cheap sparse least-squares problem. We motivate our algorithm by its theoretical analysis for the simplified case of a rank-1 matrix. Empirically, **R2RILS** is able to recover ill conditioned low rank matrices from very few observations – near the information limit, and it is stable to additive noise.

1 Introduction

Consider the following matrix completion problem, whereby the goal is to estimate an unknown $m \times n$ matrix X_0 given only few of its entries, possibly corrupted by noise. For this problem to be well posed, following many previous works, we assume that the underlying matrix X_0 is exactly of rank r , with $r \ll \min(m, n)$ and that it satisfies incoherence conditions as detailed below. For simplicity we further assume that the rank r is a-priori known. Formally, let $\Omega \subset [m] \times [n]$ be the subset of observed indices, and X the matrix with observed entries in Ω and zero in its complement Ω^c . For any matrix A , denote $\|A\|_{F(\Omega)}^2 = \sum_{(i,j) \in \Omega} A_{ij}^2$, with a similar definition for $\|A\|_{F(\Omega^c)}$. Then, the problem is

$$\min_Z \|Z - X\|_{F(\Omega)} \quad \text{subject to } \text{rank}(Z) \leq r. \quad (1)$$

Problem (1) is intimately related to matrix factorization and principal component analysis with missing data, which date back to the 1970's [Wiberg, 1976]. Such problems appear in a variety of applications, including collaborative filtering, global positioning in wireless sensor networks, system identification and structure from motion, see [Buchanan and Fitzgibbon, 2005, Candès and Plan, 2010, Davenport and Romberg, 2016] and references therein. In some applications, such as global positioning and structure from motion, the underlying matrix is exactly low rank, though the measurements may be corrupted by noise. In other applications, such as collaborative filtering,

*Faculty of Mathematics and Computer Science, Weizmann Institute of Science
(jonathan.bauch@weizmann.ac.il, boaz.nadler@weizmann.ac.il, pizilber@gmail.com)

the underlying matrix is only approximately low rank. For the vast literature on low rank matrix completion, see the reviews [Candès and Plan, 2010, Chi and Li, 2019, Chi et al., 2019, Davenport and Romberg, 2016].

In this work we focus on recovery of matrices with an *exact* rank r . For an $m \times n$ matrix X_0 of rank r , we denote its non-zero singular values by $\sigma_1 \geq \sigma_2 \geq \dots \geq \sigma_r > 0$, and its condition number by σ_1/σ_r . On the theoretical front, several works studied perfect recovery of a rank r matrix X_0 from only few entries. A key property allowing the recovery of X_0 is *incoherence* of its row and column subspaces [Candès and Recht, 2009, Candès and Tao, 2010, Gross, 2011]. The ability to recover a low rank matrix is also related to rigidity theory [Singer and Cucuringu, 2010]. Regarding the set Ω , a necessary condition for well-posedness of the matrix completion problem (1) is that $|\Omega| \geq r \cdot (m + n - r)$ which is the number of free parameters for a rank r matrix. Another necessary condition is that the set Ω contains at least r entries in each row and column [Pimentel-Alarcón et al., 2016]. When the entries of Ω are sampled uniformly at random, as few as $O(r(m+n)\text{polylog}(m+n))$ entries suffice to exactly recover an incoherent rank r matrix X_0 . For a given set Ω , we denote its oversampling ratio by $\rho = \frac{|\Omega|}{r(m+n-r)}$. In general, the closer ρ is to the value one, the harder the matrix completion task is.

On the algorithmic side, most methods for low rank matrix completion can be assigned to one of two classes. One class consists of algorithms which optimize over the full $m \times n$ matrix, whereas the second class consists of methods that explicitly enforce the rank r constraint in (1). Several methods in the first class replace the rank constraint by a low-rank inducing penalty $g(Z)$. In the absence of noise, this leads to the following optimization problem,

$$\min_Z g(Z) \quad \text{such that } Z_{ij} = X_{ij} \quad \forall (i, j) \in \Omega. \quad (2)$$

When the observed entries are noisy a popular objective is

$$\min_Z \|Z - X\|_{F(\Omega)}^2 + \lambda g(Z), \quad (3)$$

where the parameter λ is often tuned via some cross-validation procedure.

Perhaps the most popular penalty is the nuclear norm, also known as the trace norm, and given by $g(Z) = \sum_i \sigma_i(Z)$, where $\sigma_i(Z)$ are the singular values of Z [Fazel et al., 2001]. As this penalty is convex, both (2) and (3) lead to convex semi-definite programs, which may be solved in polynomial time. However, even for modest-sized matrices with hundreds of rows and columns, standard solvers have prohibitively long runtimes. Hence, several works proposed fast optimization methods, see [Avron et al., 2012, Cai et al., 2010, Fornasier et al., 2011, Ji and Ye, 2009, Ma et al., 2011, Mazumder et al., 2010, Rennie and Srebro, 2005, Toh and Yun, 2010] and references therein. On the theoretical side, under suitable conditions and with a sufficient number of observed entries, nuclear norm minimization provably recovers, with high probability, the underlying low rank matrix and is also stable to additive noise in the observed entries [Candès and Plan, 2010, Candès and Recht, 2009, Candès and Tao, 2010, Gross, 2011, Recht, 2011].

As noted by [Tanner and Wei, 2013], the nuclear norm penalty fails to recover low rank matrices at low oversampling ratios. Recovery in such data-poor settings is possible using non-convex matrix penalties such as the Schatten p -norm with $p < 1$ [Marjanovic and Solo, 2012, Kümmerle and Sigl, 2018]. However, optimizing such norms may be computationally demanding. Figure 1 compares the runtime and recovery error of HM-IRLS optimizing the Schatten p -norm with $p = 1/2$ [Kümmerle and Sigl, 2018] and of our proposed method R2RILS, as a function of matrix size m with $n = m+100$.

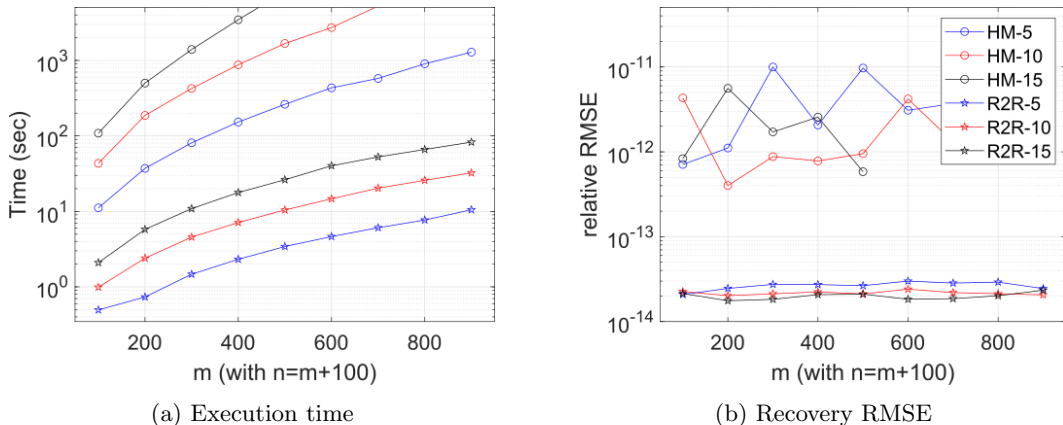


Figure 1: Comparison of HM-IRLS [Kümmerle and Sigl, 2018] and R2RILS for completion of rank r matrices of size $m \times (m + 100)$ as a function of m , at an oversampling ratio of $\rho = 2.5$. For each $r \in \{5, 10, 15\}$, all non-zero singular values were one. (a) runtime; (b) Relative RMSE on the unobserved entries, Eq. (8). Note that the y -axis in both graphs is logarithmic. Results of HM-IRLS at large values of m are not shown, as we capped individual runs to 3 hours.

For example, for a rank-10 matrix of size 700×800 , HM-IRLS required over 5000 seconds, whereas R2RILS took about 20 seconds.

The second class consists of iterative methods that strictly enforce the rank r constraint of Eq. (1). This includes hard thresholding methods that keep at each iteration only the top r singular values and vectors [Tanner and Wei, 2013, Blanchard et al., 2015, Kyrillidis and Cevher, 2014]. More related to our work are methods based on a rank r factorization $Z = UV^T$ where $U \in \mathbb{R}^{m \times r}$ and $V \in \mathbb{R}^{n \times r}$. Problem (1) now reads

$$\min_{U, V} \|UV^T - X\|_{F(\Omega)}. \quad (4)$$

Whereas Eq. (3) involves mn optimization variables, problem (4) involves only $r(m + n)$ variables, making it scalable to large matrices.

One approach to optimize Eq. (4) is by *alternating minimization* [Haldar and Hernando, 2009, Keshavan et al., 2010, Tanner and Wei, 2016, Wen et al., 2012]. Each iteration first solves a least squares problem for V , keeping the column space estimate U fixed. Next, keeping the new V fixed, it optimizes over U . Under suitable conditions, alternating minimization provably recovers the low rank matrix, with high probability [Hardt, 2014, Jain and Netrapalli, 2015, Jain et al., 2013, Keshavan et al., 2010, Sun and Luo, 2016].

Another iterative approach to optimize (4) was proposed in the 1970's by Wiberg [Wiberg, 1976], and later became popular in the computer vision community. Given a guess V^t , let $U(V^t)$ be the closed form solution to the alternating step of minimizing (4) with respect to U . Wiberg's method writes the new V as $V = V^t + \Delta V$, and performs a Newton approximation to the functional $\|U(V)V^T - X\|_{F(\Omega)}$. This yields a degenerate least squares problem for ΔV . In [Okatani et al., 2011], a damped Wiberg method was proposed with improved convergence and speed.

Yet a different approach to minimize Eq. (4) is via gradient-based Riemannian manifold optimization [Vandereycken, 2013, Boumal and Absil, 2015, Mishra and Sepulchre, 2014, Mishra et al.,

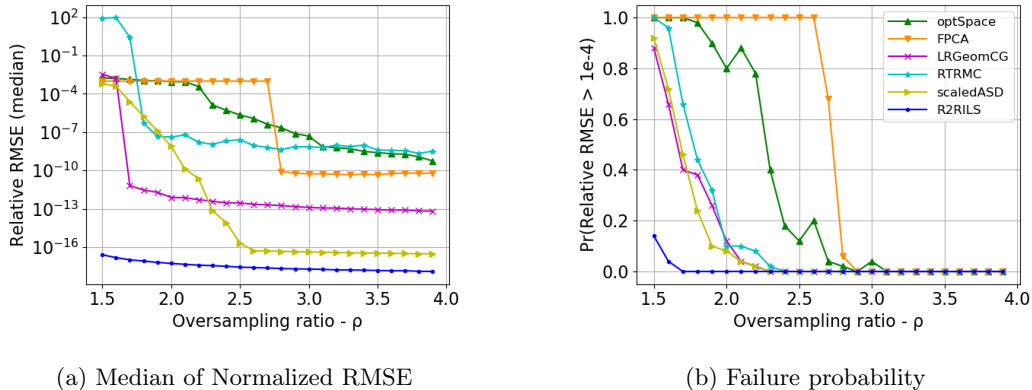


Figure 2: Comparison of several matrix completion algorithms with well-conditioned matrices of size 1000×1000 and rank $r = 5$ as a function of the oversampling ratio ρ . (a) median of rel-RMSE , Eq. (8); (b) failure probability, defined as $\text{rel-RMSE} > 10^{-4}$. Each point on the two graphs corresponds to 50 independent realizations.

2014, Ngo and Saad, 2012]. For recovery guarantees of such methods, see [Wei et al., 2016]. For scalability to large matrices, [Balzano et al., 2010] devised a stochastic gradient descent approach, called GROUSE, whereas [Recht and Ré, 2013] devised a parallel scheme called JELLYFISH. Finally, uncertainty quantification in noisy matrix completion was recently addressed in [Chen et al., 2019].

While factorization-based methods are fast and scalable, they have two limitations: (i) several of them fail to recover even mildly ill-conditioned low rank matrices and (ii) they require relatively large oversampling ratios to succeed. In applications, the underlying matrices may have a significant spread in their singular values, and clearly the ability to recover a low rank matrix from even a factor of two fewer observations may be of great importance.

Let us illustrate these two issues. With a full description in Section 3, Figure 2 shows that with a condition number of 1, several popular algorithms recover the low rank matrix. However, as shown in Figure 3, once the condition number is 10, many algorithms either require a high oversampling ratio, or fail to recover the matrix to high accuracy. In contrast, R2RILS recovers the low rank matrices from fewer entries and is less sensitive to the ill conditioning.

Our Contributions In this paper, we present R2RILS, a novel iterative method for matrix completion that is simple to implement, computationally efficient, scalable and performs well both with few observations, ill conditioned matrices and noise. Described in Section 2, R2RILS is inspired by factorization algorithms. However, it substantially differs from them, since given a target rank r , it does not directly optimize Eq. (4). Instead, we allow our interim matrix to have a specific over-parametrized rank $2r$ structure. Optimizing over this rank $2r$ matrix yields a least squares problem. At each iteration, R2RILS thus simultaneously optimizes the column and row subspaces. A key step is then an *averaging* of these new and current estimates.

Section 3 presents an empirical evaluation of R2RILS. First, we consider rank r incoherent matrices, with entries observed uniformly at random. We show that in noise-free settings, R2RILS exactly completes matrices from fewer entries than several other low rank completion methods. We further show that R2RILS is robust to ill-conditioning of the underlying matrix and to additive noise.

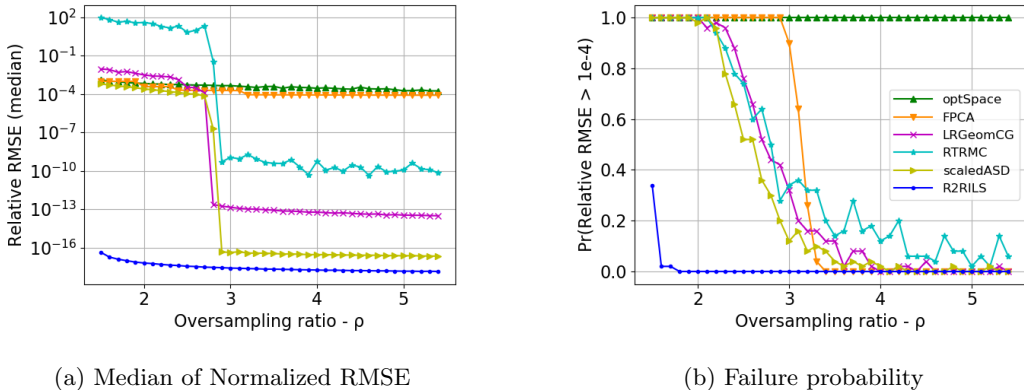


Figure 3: Similar comparison as in Fig. 2, but now the rank 5 matrices have singular values 10, 8, 4, 2, 1, resulting in a condition number of 10.

Next, we consider a different type of ill-conditioning, namely power-law matrices which are much less incoherent. Finally, we compare R2RILS to the damped Wiberg’s algorithm on two datasets from computer vision, where the later method was shown to obtain state-of-the-art results. This comparison also highlights some limitations of our method.

To provide insight and motivation for our approach, in Section 4 we study some of its theoretical properties, under the simplified setting of a rank-1 matrix, both with noise free observations as well as with observations corrupted by additive Gaussian noise. While beyond the scope of the current manuscript, we remark that the approach we present in this work can be extended to several other problems, including Poisson low rank matrix completion, one bit matrix completion, and low rank tensor completion. These will be described in future works.

2 The R2RILS Algorithm

While motivated by factorization methods, a key difference of R2RILS is that it does not directly optimize the objective of Eq. (4). Instead, R2RILS utilizes a specific *lifting* to the space of rank $2r$ matrices. Let (U_t, V_t) be the estimates of the column and row spaces of the rank r matrix X_0 , at the start of iteration t . Consider the subspace of rank $2r$ matrices of the following specific form, with $A \in \mathbb{R}^{m \times r}$, $B \in \mathbb{R}^{n \times r}$.

$$U_t B^\top + A V_t^\top,$$

Starting from an initial guess (U_1, V_1) at $t = 1$, R2RILS iterates the following two steps:

Step I. Compute the minimal ℓ_2 -norm solution $(\tilde{U}_t, \tilde{V}_t)$ of the following least squares problem

$$\operatorname{argmin}_{A \in \mathbb{R}^{m \times r}, B \in \mathbb{R}^{n \times r}} \|U_t B^\top + A V_t^\top - X\|_{F(\Omega)}. \quad (5)$$

Algorithm 1: R2RILS

Input : Ω - the set of observed entries.
 X - an $m \times n$ matrix with the observed values in Ω and zeros in Ω^c ,
 r - the target rank
 U_1, V_1 - initial guess for the column and row rank- r subspaces
 t_{\max} - maximal number of iterations

Output: \hat{X} - rank r approximation of X

- 1 **for** $t = 1, \dots, t_{\max}$ **do**
- 2 Compute $(\tilde{U}_t, \tilde{V}_t)$, the minimal norm solution of

$$\operatorname{argmin}_{A \in \mathbb{R}^{m \times r}, B \in \mathbb{R}^{n \times r}} \|U_t B^\top + A V_t^\top - X\|_{F(\Omega)}$$
- 3 $U_{t+1} = \operatorname{ColNorm}\left(U_t + \operatorname{ColNorm}\left(\tilde{U}_t\right)\right)$
- 4 $V_{t+1} = \operatorname{ColNorm}\left(V_t + \operatorname{ColNorm}\left(\tilde{V}_t\right)\right)$
- 5 **end**
- 6 **return** $\hat{X} = \text{rank } r$ approximation of $(U_t \tilde{V}_t^\top + \tilde{U}_t V_t^\top)$ at the iteration t which achieved the smallest squared error on the observed entries

Step II. Update the row and column subspace estimates,

$$\begin{aligned} U_{t+1} &= \operatorname{ColNorm}\left(U_t + \operatorname{ColNorm}\left(\tilde{U}_t\right)\right), \\ V_{t+1} &= \operatorname{ColNorm}\left(V_t + \operatorname{ColNorm}\left(\tilde{V}_t\right)\right), \end{aligned} \tag{6}$$

where $\operatorname{ColNorm}(A)$ normalizes all r columns of the matrix A to have unit norm.

At each iteration we compute the rank r projection of the rank- $2r$ matrix $U_t \tilde{V}_t^\top + \tilde{U}_t V_t^\top$ and its squared error on the observed entries. The output of R2RILS is the rank r approximation of $(U_t \tilde{V}_t^\top + \tilde{U}_t V_t^\top)$ which minimizes the squared error on the observed entries. A pseudo-code of R2RILS appears in Algorithm 1. As we prove in Lemma 2, if R2RILS converges, then its limiting solution is rank r . Next, we provide intuition for R2RILS and discuss some of its differences from other factorization-based methods.

Rank Deficiency. As discussed in Lemma 1 below, Eq. (5) is a rank deficient least squares problem and therefore does not have a unique solution. R2RILS takes the solution with smallest Euclidean norm, which is unique. We remark that the least squares linear system in Wiberg’s method, although different, has a similar rank deficiency, see [Okatani and Deguchi, 2007, Proposition 1].

Simultaneous Row and Column Optimization. In Eq. (5) of Step I, R2RILS finds the best approximation of X by a linear combination of the current row and column subspace estimates (U_t, V_t) , using weight matrices (A, B) . Thus, Eq. (5) *simultaneously* optimizes both the column and row subspaces, generating new estimates for them $(\tilde{U}_t, \tilde{V}_t)$. This scheme is significantly different from alternating minimization methods, which at each step optimize only one of the row or column subspaces, keeping the other fixed. In contrast, R2RILS *decouples* the estimates, at the expense of lifting to a rank $2r$ intermediate solution,

$$\hat{X}_t = U_t \tilde{V}_t^\top + \tilde{U}_t V_t^\top. \tag{7}$$

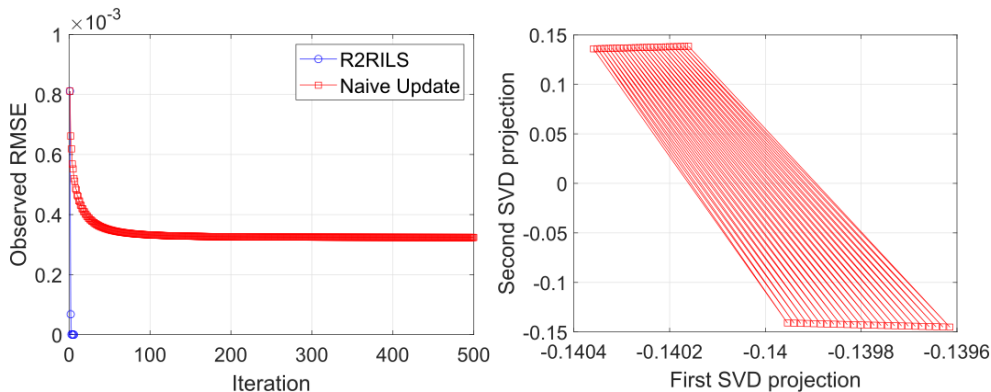


Figure 4: Comparison of R2RILS versus a variant with a naive update. The input is a 400×500 matrix of rank $r = 3$, with observed entries uniformly at random at an oversampling ratio $\rho = 5$. (a) Observed RMSE as a function of iteration counter. (b) Two dimensional visualization of the oscillating dynamics of U_t under the naive update rule.

Tangent Space. Another prism to look at Eq. (5) is through its connection to the tangent space of the manifold of rank r matrices. Consider a rank r matrix with column and row subspaces spanned by U_t, V_t , i.e. $Z = U_t M V_t^T$ where $M \in \mathbb{R}^{r \times r}$ is invertible. Then the rank $2r$ matrix of Eq. (7) is the best approximation of X in the *tangent space* of Z , in least squares sense.

Averaging Current and New Estimates. Since $(\tilde{U}_t, \tilde{V}_t)$ can be thought of as new estimates for the column and row spaces, it is tempting to consider the update $U_{t+1} = \tilde{U}_t, V_{t+1} = \tilde{V}_t$, followed by column normalization. While this update may seem attractive, leading to a non increasing sequence of losses for the objective in Eq. (5), it performs very poorly. Empirically, this update decreases the objective in Eq. (5) extremely slowly, taking thousands of iterations to converge. Moreover, as illustrated in Figure 4, the resulting sequence $\{(U_t, V_t)\}_t$ alternates between two sets of poor estimates. The left panel shows the RMSE on the observed entries versus iteration number for R2RILS, and for a variant whose update is $U_{t+1} = \tilde{U}_t, V_{t+1} = \tilde{V}_t$, followed by column normalization. Both methods were initialized by the SVD of X . While R2RILS converged in 6 iterations, the naive method failed to converge even after 500 iterations. The right panel presents a 2-d visualization of the last 50 vectors $U_{t,1}$ under the naive update, as projected into the first and second SVD components of the matrix containing the last 50 values of U_t for $t = 451 : 500$. This graph shows an oscillating behavior between two poor vectors. Remark 2 explains this behavior, in the rank-one case.

Nonetheless, thinking of $(\tilde{U}_t, \tilde{V}_t)$ as new estimates provides a useful perspective. In particular, if the error in $(\tilde{U}_t, \tilde{V}_t)$ is in a different direction than the error in the initial estimate (U_t, V_t) or better yet, is approximately in the *opposite* direction, then the sensible operation to perform is to *average* these two estimates. This is indeed what R2RILS does in its second step. In Section 4 we show that in the rank-1 case, when the entire matrix is observed, the errors in $(\tilde{U}_t, \tilde{V}_t)$ are indeed approximately in the opposite direction. Furthermore, we show that when the previous estimates are already close to the ground truth, the equal weighting of previous and current estimates is asymptotically optimal. Specifically, this averaging cancels the leading order terms of the errors, and leads to quadratic convergence.

Non-Local Updates. Several Riemannian optimization methods, such as LRGeomCG [Vandereyken, 2013] and RTRMC [Boumal and Absil, 2015], perform *local* optimization on the manifold of rank r matrices, based on the gradient at the current solution. Our update rule is significantly different from these methods, since in Step I, we find the *global* minimizer of Eq. (5) in a specific rank $2r$ subspace. Given the averaging operation in the second step of R2RILS, its next estimate (U_{t+1}, V_{t+1}) may be far from the current one (U_t, V_t) , in particular in the first few iterations.

Invariant Alternatives. An intriguing property of R2RILS is that its next estimate depends explicitly on the specific columns of (U_t, V_t) , and not only on the subspace they span. That is, R2RILS is not invariant to the representation of the current subspace, and does not treat (U_t, V_t) as elements on the Grassmannian. It is possible to devise variants of R2RILS that are invariant to the subspace representation. One way to do so is to update (U_{t+1}, V_{t+1}) as the average subspace between (U_t, V_t) and $(\tilde{U}_t, \tilde{V}_t)$, with respect to say the standard Stiefel geometry. Another invariant alternative is to take the best rank r approximation of \hat{X}_t from (7) as the next estimate. While these variants work well at high oversampling ratios, the simple column averaging Eq. (6) outperforms them at low oversampling ratios. A theoretical understanding of this behavior is an interesting topic for future research.

Initialization. Similar to other iterative algorithms, R2RILS requires an initial guess U_1, V_1 . When the observed entries are distributed uniformly at random, a common choice is to initialize U_1, V_1 by the top r left and right singular vectors of X . As described in [Keshavan et al., 2010], for a trimmed variant of X , these quantities are an accurate estimate of the left and right subspaces. In contrast, when the distribution of the observed entries is far from uniform, the rank- r SVD of X may be a poor initialization, and in various applications, one starts from a random guess, see [Okatani et al., 2011]. Empirically, R2RILS performs well also from a random initialization, say with i.i.d. $N(0, I)$ Gaussian vectors, though it may require more iterations to converge. This suggests that the sequence (U_t, V_t) computed by R2RILS is not attracted to poor local minima. This finding is in accordance with [Ge et al., 2016], that rigorously proved lack of poor local minima for the matrix completion problem under suitable assumptions.

Early Stopping. In the pseudo-code of Algorithm 1, the number of iterations is fixed at t_{\max} . In most of our simulations, we set $t_{\max} = 300$, though in practice, the algorithm often converged in much fewer iterations. In our code we implemented several early stopping criteria. Let $\hat{X}_r^t = \text{SVD}_r(U_t \tilde{V}^\top + \tilde{U} V_t^\top)$ denote the rank- r approximation of \hat{X}_t from Eq. (7), and let $\text{RMSE}_{\text{obs}}^t = \|\hat{X}_r^t - X\|_{F(\Omega)} / \sqrt{|\Omega|}$ be the corresponding root mean squared error on the observed entries. Then the first criterion, relevant only to the noise-free case, is

$$\text{Stop if } \quad \text{RMSE}_{\text{obs}}^t \leq \epsilon,$$

taking for instance $\epsilon \leq 10^{-15}$. A second stopping criterion, valid also in the noisy case, is

$$\text{Stop if } \quad \frac{\|\hat{X}_t - \hat{X}_{t-1}\|_F}{\sqrt{mn}} \leq \epsilon.$$

Finally, a third stopping criterion, useful in particular with real data, is to set $\delta \ll 1$ and

$$\text{Stop if } \quad |\text{RMSE}_{\text{obs}}^t - \text{RMSE}_{\text{obs}}^{t-1}| \leq \delta \cdot \text{RMSE}_{\text{obs}}^t$$

Computational complexity. Our Matlab and Python implementations of R2RILS, available at the author’s website¹, use standard linear algebra packages. Specifically, the minimal norm solution of Eq. (5) is calculated by the LSQR iterative algorithm [Paige and Saunders, 1982]. The cost per iteration of LSQR is discussed in [Paige and Saunders, 1982, Section 7.7]. In our case, it is dominated by the computation of $U_t B^\top + A V_t^\top$ at all entries in Ω , whose complexity is $\mathcal{O}(r|\Omega|)$. LSQR is mathematically equivalent to conjugate gradient applied to the normal equations. As studied in [Hayami, 2018, Section 4], the residual error after k iterations decays like

$$C \left(\frac{\sigma_{\max} - \sigma_{\min}}{\sigma_{\max} + \sigma_{\min}} \right)^k,$$

where σ_{\max} and σ_{\min} are the largest and smallest non-zero singular values of the rank-deficient matrix of the least squares problem (5). Empirically, at an oversampling ratio $\rho = 2$ and matrices of size 300×300 , the above quotient is often smaller than 0.9. Thus, LSQR often requires at most a few hundreds of inner iterations to converge. For larger sized matrices and more challenging instances, more iterations may be needed for a very accurate solution. We capped the maximal number of LSQR iterations at 4000.

Attenuating Non-convergence. On challenging problem instances, where R2RILS fails to find the global minimum solution, empirically the reason is not convergence to a bad local minima. Instead, due to its global updates, (U_t, V_t) often oscillates in some orbit. To attenuate this behavior, if R2RILS did not converge within say the first 40 iterations, then once every few iterations we replace the averaging in Eq. (6) with a weighted averaging, which gives more weight to the previous estimate, of the form

$$U_{t+1} = \text{ColNorm} \left(\beta U_t + \text{ColNorm} \left(\tilde{U}_t \right) \right),$$

and a similar formula for V_{t+1} . In our simulations we took $\beta = 1 + \sqrt{2}$. Empirically, this modification increased the cases where R2RILS converged within t_{\max} iterations.

3 Numerical Results

We present simulation results that demonstrate the performance of R2RILS. In the following experiments random matrices were generated according to the uniform model. Specifically, $\{u_i\}_{i=1}^r, \{v_i\}_{i=1}^r$ were constructed by drawing r vectors uniformly at random from the unit spheres in $\mathbb{R}^m, \mathbb{R}^n$ respectively and then orthonormalizing them. At every simulation we specify the singular values $\{\sigma_i\}_{i=1}^r$ and construct the rank r matrix X_0 as

$$X_0 = \sum_{i=1}^r \sigma_i u_i v_i^T.$$

With high probability, the matrix X_0 is incoherent [Candès and Recht, 2009]. At each oversampling ratio ρ , we generate a random set Ω of observed entries by flipping a coin with probability $p = \rho \cdot \frac{r(m+n-r)}{(m \cdot n)}$ at each of the mn matrix entries. The size of Ω is thus variable and distributed as Binom($m \cdot n, p$). As in [Kümmerle and Sigl, 2018], we then verify that each column and row have

¹www.wisdom.weizmann.ac.il/~nadler/Projects/R2RILS/

at least r visible entries and repeat this process until this necessary condition for unique recovery is satisfied.

We compare **R2RILS** with maximal number of iterations $t_{\max} = 100$ to the following algorithms, using the implementations supplied by the respective authors. As detailed below, for some of them we slightly tuned their parameters to improve their performance.

- **OptSpace** [Keshavan et al., 2010]: Maximal number of iterations set to 100. Tolerance parameter 10^{-10} .
- **FPCA** [Ma et al., 2011]: Forced the implementation to use a configuration for "hard" problem where several parameters are tightened. The two tolerance parameters were set to 10^{-16} .
- **LRGeomCG** [Vandereycken, 2013]: Executed with its default parameters.
- **RTRMC** [Boumal and Absil, 2015]: Maximal number of iterations 300, maximal number of inner iterations set to 500. The gradient tolerance was set to 10^{-10} .
- **ScaledASD** [Tanner and Wei, 2016]: Tolerance parameters 10^{-14} and maximal number of iterations 1000.
- **HM-ILS** [Kümmerle and Sigl, 2018]: Executed with its default parameters.

We considered two performance measures. The first is the relative RMSE per-entry over the unobserved entries. Given an estimated matrix \hat{X} , this quantity is defined as

$$\text{rel-RMSE} = \sqrt{\frac{m \cdot n}{|\Omega^c|}} \cdot \frac{\|\hat{X} - X_0\|_{F(\Omega^c)}}{\|X_0\|_F}. \quad (8)$$

The second measure is the success probability of an algorithm in the ideal setting of noise-free observations. We define success as $\text{rel-RMSE} < 10^{-4}$. This is similar to [Tanner and Wei, 2016], who computed a relative RMSE on all matrix entries, and considered a recovery successful with a slightly looser threshold of 10^{-3} . We compare **R2RILS** to all the above algorithms except for **HM-ILS** which will be discussed separately. In addition, we also tested the **R3MC** algorithm [Mishra and Sepulchre, 2014] and the damped **Wiberg** method of [Okatani et al., 2011]. To limit the number of methods shown in the plots of Figs. 2 and 3, the performance of these two methods is not shown in these figures. However, their performance was similar to that of other Riemannian optimization based methods.

Well conditioned setting. In our first experiment, we considered a relatively easy setting with well conditioned matrices of size 1000×1000 and rank $r = 5$, whose non zero singular values were all set to 1. Figure 2 shows the reconstruction ability of various algorithms as a function of the oversampling ratio ρ . In this scenario all algorithms successfully recover the matrix once enough entries are observed. Even in this relatively easy setting, **R2RILS** shows favorable performance at low oversampling ratios, reaching a relative RMSE around 10^{-14} .

Mild ill-conditioning. Next, we consider a mild ill-conditioning setting, where the rank $r = 5$ matrices have a condition number 10, and non-zero singular values 10, 8, 4, 2, 1. As seen in Fig. 3, **R2RILS** is barely affected by this ill-conditioning and continues to recover the underlying matrix with error 10^{-14} at oversampling ratios larger than 1.5. In contrast, **FPCA**, which performs nuclear

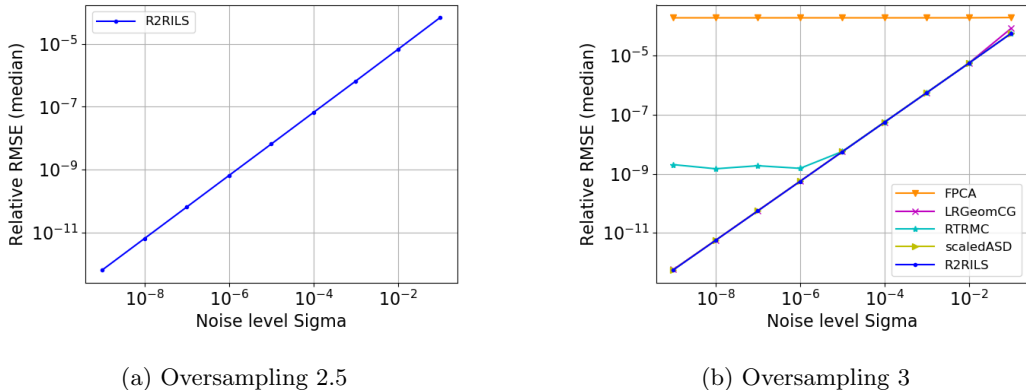


Figure 5: Comparison of several matrix completion algorithms with ill-conditioned matrices and entries corrupted by additive Gaussian noise. Matrices were drawn as in the simulations of Fig. 2. We plot the RMSE per unobserved entry as a function of the standard deviation of the noise. Each point on the graphs corresponds to 50 independent realizations.

norm minimization, recovers the matrix at higher oversampling ratios $\rho > 3.4$. This is in accordance to similar observations by previous works [Tanner and Wei, 2013, Kümmerle and Sigl, 2018]. The other compared algorithms, all of which solve non-convex problems, also require higher oversampling ratios than R2RILS, and even then, occasionally fail to achieve a relative RMSE less than 10^{-4} .

Comparison to HM-ILS. The HM-ILS algorithm [Kümmerle and Sigl, 2018] was not included in the above simulations due to its slow runtime. However, from a limited evaluation with smaller sized matrices HM-ILS with Schatten p -norm parameter $p = 1/2$ has excellent performance, comparable to R2RILS, also under ill-conditioning. Figure 1b demonstrates that at a low oversampling ratio $\rho = 2.5$, both algorithms perfectly reconstruct matrices of various dimensions. Figure 1a shows that R2RILS is faster than HM-ILS by orders of magnitude even for modestly sized matrices.

Comparison to Riemannian Manifold Optimization Methods. We considered the optimization path as well as the output of the LRGeomCG algorithm on an instance where it failed to exactly complete the matrix within an increased number of 20000 iterations. Figure 6 shows the norm of the gradient and the normalized error on the observed entries of LRGeomCG versus iteration count. On this instance, the normalized error on the observed entries was 0.0241, whereas on the unobserved entries it was 9.11. It seems that at low oversampling ratios, LRGeomCG converges very slowly to a bad local optimum. Interestingly, starting from this solution of LRGeomCG, R2RILS recovers the low rank matrix within only 20 iterations, with an RMSE of 10^{-13} . We observed the same behavior for 10 different matrices. It thus seems that the lifting to a rank $2r$ matrix leads to fewer bad local minima in the optimization landscape. A theoretical study of this issue is an interesting topic for further research.

Stability to Noise. Figure 5 illustrates the performance of several matrix completion algorithms when i.i.d. zero mean Gaussian noise is added to every observed entry of X_0 . As seen in panel 5a, R2RILS is robust to noise even at low oversampling ratios, with the RMSE linear in the noise level.

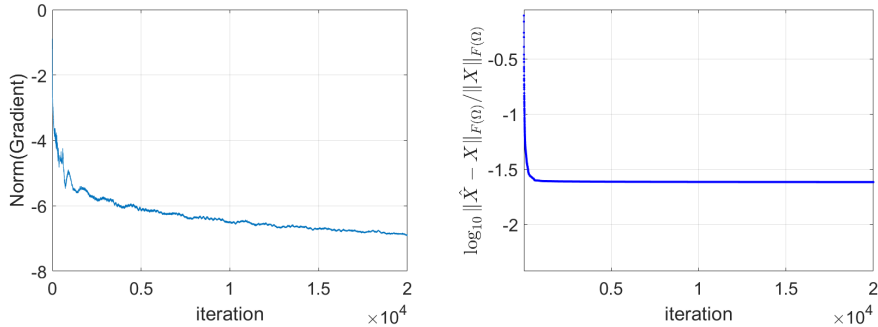


Figure 6: Typical optimization path of LRGeomCG on a 1000×1000 matrix of rank $r = 5$, condition number 10, at oversampling ratio $\rho = 2.2$. (Left) The norm of the gradient at each iteration on a logarithmic scale. (Right) The normalized error on the observed entries.

In Section 4, we prove this result in the case of a fully observed rank-1 matrix. Panel 5b shows that most algorithms are also robust to noise, but only at higher oversampling ratios where they start to work in the absence of noise. Algorithms that even without noise failed to recover at an oversampling ratio $\rho = 3$ are not included in this graph.

Convergence Rate. Figure 7 illustrates the relative RMSE of R2RILS per observed entry, Eq. (8), as a function of the iteration number, on two rank-5 matrices of dimension 1000×1000 , oversampling ratio 2.5 and condition numbers 1 and 10. It can be observed that R2RILS’s convergence is very quick once it reaches a small enough error. It is also interesting to note that R2RILS does not monotonically decrease the objective in Eq. (5) at every iteration.

Power-law Matrices. Another form of ill conditioning occurs when the row and/or column subspaces are only weakly incoherent. As in [Chen et al., 2015], we consider power-law matrices of the form $X = DUV^T D$ where the entries of U and V are i.i.d. $\mathcal{N}(0, 1)$ and $D = D(\alpha)$ is a diagonal matrix with power-law decay, $D_{ii} = i^{-\alpha}$. When $\alpha = 0$ the matrix is highly incoherent and relatively easy to recover. When $\alpha = 1$ it is highly coherent and more difficult to complete from few entries. Given a budget on the number of observed entries, a 2-step sampling scheme was proposed in [Chen et al., 2015]. As shown in [Chen et al., 2015, Fig. 1], $10n \log(n)$ adaptively chosen samples were sufficient to recover rank-5 matrices of size 500×500 by nuclear norm minimization, for values of $\alpha \leq 0.9$. In contrast, with entries observed uniformly at random, nuclear norm minimization required over $300n \log(n)$ entries for $\alpha \geq 0.8$. Figure 8 shows the rate of successful recovery (as in [Chen et al., 2015], defined as $\|\hat{X} - X\|_F / \|X\|_F \leq 0.01$) by R2RILS as a function of number of entries, chosen uniformly at random while only verifying that each row and column has at least $r = 5$ entries. As seen in the figure, R2RILS recovers the underlying matrices with less than $10n \log(n)$ entries up to $\alpha = 0.8$, namely without requiring sophisticated adaptive sampling.

Datasets from Computer Vision. We conclude the experimental section with results on two benchmark datasets² from the computer vision literature [Buchanan and Fitzgibbon, 2005,

²Datasets available at <https://github.com/jhh37/lrmf-datasets/find/master>

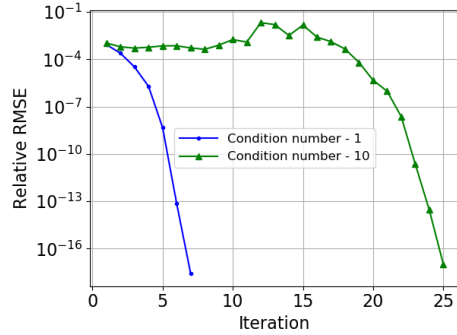


Figure 7: Relative RMSE per *observed* entry of R2RILS as a function of the iteration number. Each line represents a single execution of R2RILS on a 1000×1000 rank-5 matrix, with oversampling ratio $\rho = 2.5$. For the condition-1 matrix all non-zero singular values were set to 1. For the matrix with condition number-10 singular values were set to 10, 8, 4, 2, 1.

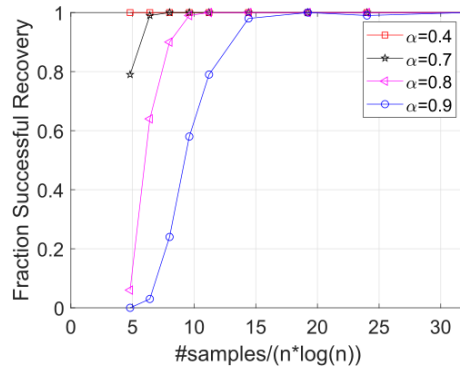


Figure 8: Recovery of power-law matrices by R2RILS.

[Hyeong Hong and Fitzgibbon, 2015]. We compare R2RILS with the **damped Wiberg** method³, which is one of the top performing methods on these benchmarks [Okatani et al., 2011]. In these datasets, the goal is to construct a matrix \hat{X} of given rank r , whose RMSE at the observed entries is as small as possible. The observed indices are structured. Hence, the SVD of the observed matrix does not provide an accurate initial guess. Instead, it is common to initialize methods with random U and V , whose entries are i.i.d. $\mathcal{N}(0, 1)$. The quality of an algorithm is assessed by its ability to converge to a solution with low observed RMSE, and by the number of iterations and overall clock time it takes to do so, see [Hyeong Hong and Fitzgibbon, 2015].

The first dataset is Din (Dino Trimmed in [Hyeong Hong and Fitzgibbon, 2015]), involving the recovery of the rigid turntable motion of a toy dinosaur. The task is to fit a rank $r = 4$ matrix of size 72×319 , given 5302 observed entries (23.1%). The best known solution has RMSE 1.084673, and condition number 12.4. Starting from a random guess, R2RILS with maximal number of iterations

³Code downloaded from <http://www.vision.is.tohoku.ac.jp/us/download/>. The method was run with default parameters as suggested in [Okatani et al., 2011].

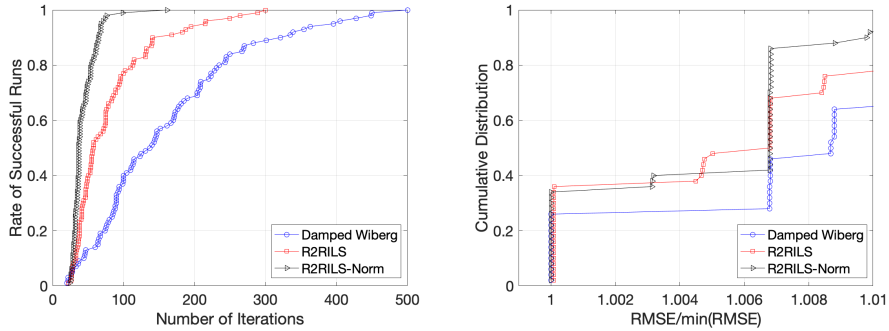


Figure 9: (Left) Cumulative distribution for number of iterations to converge to optimal solution on Din dataset. (Right) Cumulative Distribution of the observed RMSE per entry, divided by the minimal RMSE, on the UB4 dataset, from 50 different random initializations.

$t_{\max} = 300$ achieved this objective in 99/100 runs. The least squares system that R2RILS has to solve is very ill-conditioned for this dataset. We thus also considered a variant, whereby we normalized the columns of the least squares matrix to have unit norm. This variant attained the optimal objective in all 100 runs, and on average converged in fewer number of iterations. Figure 9 (left) shows the cumulative rate of attaining this objective for the three tested algorithms.

The second dataset is UB4 (Um-boy). Here the task is to fit a rank $r = 4$ matrix of size 110×1760 given 14.4% of its entries. The best known solution has observed RMSE 1.266484 and condition number 24.5. Out of 50 runs, **damped Wiberg** attained this RMSE in 13 cases, and the normalized R2RILS variant in 17 runs. The lowest RMSE obtained by R2RILS was slightly higher (1.266597) and this occurred in 18 cases. This suggests that R2RILS may be improved by preconditioning the linear system. A practically important remark is that in these datasets, each iteration of **damped Wiberg** is significantly faster, as it solves a linear system with only $r \min(m, n)$ variables, compared to $r(m + n)$ for R2RILS. On the Din dataset, since the ratio $n/m \approx 4.4$, the mean runtime of the normalized variant is only slightly slower than that of **damped Wiberg**, 17 seconds versus 11 seconds. However, on the UB4 dataset, where $n/m = 16$, the clock time of **damped Wiberg** is significantly faster by a factor of about 60. Developing a variant of R2RILS that solves only for the smaller dimension and would thus be much faster, is an interesting topic for future research.

4 Theoretical Analysis

We present a preliminary theoretical analysis, which provides both motivation and insight into the two steps of R2RILS. First, Lemma 1 shows that the least squares problem (5) has rank deficiency of dimension at least r^2 , similar to Wiberg’s algorithm [Okatani and Deguchi, 2007, Proposition 1]. Next, even though R2RILS lifts to rank $2r$ matrices, Lemma 2 shows that if it converges, the limiting solution is in fact of rank r . Hence, if this solution attains a value of zero for the objective (5), then R2RILS outputs the true underlying matrix X_0 . Finally, we study the convergence of R2RILS in the simple rank-1 case. Assuming that the entire matrix is observed, we prove in Theorem 1 that starting from any initial guess weakly correlated to the true singular vectors, R2RILS converges linearly to the underlying matrix. Its proof motivates the averaging step of R2RILS, as it shows that

in the rank-1 case, the errors of $(\tilde{U}_t, \tilde{V}_t)$ relative to the true singular vectors are approximately in the *opposite* direction compared to the errors in (U_t, V_t) . Using this property, we show in Theorem 2 that locally, the convergence of R2RILS is quadratic. Remarks 2 and 3 provide insight and theoretical justification for the equal weighting in the averaging step (6), as well as the choice of the minimal norm solution to the least squares problem (5). Finally, Theorem 3 shows that R2RILS is stable to additive noise, in the fully observed rank-1 case.

Lemma 1. *Suppose that the r columns of U_t and of V_t are both linearly independent. Then, the solution space of Eq. (5) has dimension at least r^2 . In addition, in the rank-1 case, when $\Omega = [m] \times [n]$ the solution space has dimension exactly 1.*

Proof. The solution of (5) is unique up to the kernel of the linear map

$$(A, B) \mapsto \text{Vec}_\Omega (U_t B^\top + A V_t^\top) = \text{Vec}_\Omega \left(\sum_{i=1}^r (U_t)_i b_i^\top + a_i (V_t)_i^\top \right), \quad (9)$$

where $(U_t)_i$ denotes the i -th column of U and $\text{Vec}_\Omega(B) \in \mathbb{R}^{|\Omega|}$ is a vector with entries $B_{i,j}$ for $(i, j) \in \Omega$. Choosing $a_i = \sum_{j=1}^r \lambda_{i,j} (U_t)_j$ and $b_i = -\sum_{j=1}^r \lambda_{j,i} (V_t)_j$ with r^2 free parameters $\lambda_{i,j}$ yields an element of the kernel. Hence, the dimension of the kernel is at least r^2 .

As for the second part of the lemma, suppose that (a, b) is a non-trivial solution, such that

$$u_t b^\top + a v_t^\top = 0. \quad (10)$$

Then $\exists i$ such that $b_i \neq 0$ and by Eq. (10) $b_i u_t = -(v_t)_i a$, implying that $a \in \text{Span}\{u_t\}$. A similar argument shows that $b \in \text{Span}\{v_t\}$. Hence the two terms in Eq. (10) take the form $u_t b^\top = \lambda_1 u_t v_t^\top$ and $a v_t^\top = \lambda_2 u_t v_t^\top$ for some $\lambda_1, \lambda_2 \in \mathbb{R}$. For Eq. (10) to hold, $\lambda_1 = -\lambda_2$. Thus, any non trivial solution belongs to the rank-1 subspace $\lambda(u_t, -v_t)$. \square

Lemma 2. *Let \mathcal{M}_r be the manifold of $m \times n$ rank r matrices. Denote by $L : \mathcal{M}_r \rightarrow \mathbb{R}$ the squared error loss on the observed entries,*

$$L(Z) = \|Z - X\|_{F(\Omega)}^2.$$

Suppose that (U_t, V_t) is a fixed point of R2RILS, and that the r columns of U_t and of V_t are both linearly independent. Then the rank $2r$ matrix \hat{X}_t is rank r and is a critical point of L .

Proof. Suppose (U_t, V_t) is a fixed point of R2RILS. Then the solution $(\tilde{U}_t, \tilde{V}_t)$ of Eq. (5) can be written as follows, with diagonal matrices $\Sigma_U, \Sigma_V \in \mathbb{R}^{r \times r}$,

$$(\tilde{U}_t, \tilde{V}_t) = (U_t \Sigma_U, V_t \Sigma_V)$$

This implies that R2RILS's interim rank $2r$ estimate \hat{X}_t of Eq. (7) is in fact of rank r , since

$$\hat{X}_t = U_t \Sigma_V^\top V_t^\top + U_t \Sigma_U V_t^\top = U_t (\Sigma_U + \Sigma_V^\top) V_t^\top.$$

The rank r matrix \hat{X}_t is a critical point of the function L on the manifold \mathcal{M}_r if and only if its gradient ∇L is orthogonal to the tangent space at \hat{X}_t , denoted $T_{\hat{X}_t} \mathcal{M}_r$. Suppose by contradiction that \hat{X}_t is not a critical point of L on \mathcal{M}_r . Equivalently,

$$\nabla L(\hat{X}_t) \not\perp T_{\hat{X}_t} \mathcal{M}_r. \quad (11)$$

The gradient of the loss L at a point Z is given by $\nabla L(Z) = 2(P_\Omega(Z) - X)$ where P_Ω is the projection operator onto the observed entries in the set Ω ,

$$(P_\Omega(Z))_{i,j} = \begin{cases} Z_{i,j}, & \text{if } (i,j) \in \Omega, \\ 0, & \text{otherwise.} \end{cases}$$

The tangent space at a point $Z = U\Sigma V^\top \in \mathcal{M}_r$, where Σ is an invertible $r \times r$ matrix, is given by [Vandereycken, 2013, Proposition 2.1]

$$T_Z \mathcal{M}_r = \{UB^\top + AV^\top \mid A \in \mathbb{R}^{m \times r}, B \in \mathbb{R}^{n \times r}\}.$$

Eq. (11) means that the projection of $\nabla L(\hat{X}_t)$ onto the tangent space $T_{\hat{X}_t} \mathcal{M}$ is non trivial. Let $U_t B^\top + AV_t^\top$ be this projection. Then

$$\|P_\Omega(\hat{X}_t) - X - U_t B^\top - AV_t^\top\|_F < \|P_\Omega(\hat{X}_t) - X\|_F.$$

Since $P_\Omega(\hat{X}_t)$ and X both vanish on Ω^c , the right hand side equals $\|P_\Omega(\hat{X}_t) - X\|_{F(\Omega)}$. Thus,

$$\|P_\Omega(\hat{X}_t) - X - U_t B^\top - AV_t^\top\|_{F(\Omega)} \leq \|P_\Omega(\hat{X}_t) - X - U_t B^\top - AV_t^\top\|_F < \|P_\Omega(\hat{X}_t) - X\|_{F(\Omega)}.$$

This contradicts the assumption that $(\tilde{U}_t, \tilde{V}_t)$ is a global minimizer of Eq. (5). \square

Corollary 1. *Consider a noise-free matrix completion problem with an underlying matrix X_0 of rank r and a set $\Omega \subset [m] \times [n]$ such that the solution to (1) is unique. If **R2RILS** converged to a fixed point (U_t, V_t) with a zero value for the least squares objective (5), $\|U_t \tilde{V}_t^\top + \tilde{U}_t V_t^\top - X\|_{F(\Omega)} = 0$, then its output is the true underlying matrix X_0 .*

Proof. By Lemma 2, if **R2RILS** converged then the intermediate matrix $U_t \tilde{V}_t^\top + \tilde{U}_t V_t^\top$ is in fact rank- r . As this matrix attains a zero value for the objective (1), it equals X_0 . \square

Next, we study the convergence of **R2RILS**, in the simple case where $X_0 = \sigma uv^\top$ is of rank-1, and assume that we have observed *all* entries of X_0 . These two assumptions allow us to find a closed form solution to the least squares problem and are critical for our proof analysis. It may be possible to extend our proof to higher rank settings and to partially observed matrices with a more complicated proof. We leave this for future work.

Let (u_t, v_t) be the estimates of **R2RILS** at iteration t . In the rank-1 case u_t and v_t are vectors and we may decompose each of them into two components. The first is their projection on the true (u, v) , and the second is the orthogonal complement which is their error,

$$u_t = \alpha_t u + \sqrt{1 - \alpha_t^2} e_{u,t}, \quad v_t = \beta_t v + \sqrt{1 - \beta_t^2} e_{v,t}. \quad (12)$$

For future use we define $\epsilon_t = \sqrt{1 - \alpha_t^2}$, $\delta_t = \sqrt{1 - \beta_t^2}$, and the following two quantities

$$h(\epsilon) = \sqrt{1 + 2\epsilon^2 - 3\epsilon^4}, \quad r(\epsilon) = \frac{1 + \epsilon^2 + h(\epsilon)}{\sqrt{2(1 + 3\epsilon^2 + h(\epsilon))}}. \quad (13)$$

Note that both (u, v) and hence also (α_t, β_t) are determined up a joint ± 1 sign. In the following, we will assume that the initial guess satisfies $\text{sign}(\alpha_1) = \text{sign}(\beta_1) > 0$.

The first theorem below shows that in the fully-observed rank-1 case, from any initial guess weakly correlated to the true singular vectors $(\alpha_1, \beta_1 > 0)$, **R2RILS** converges linearly to the matrix X_0 . The second theorem shows that asymptotically, the convergence is quadratic.

Theorem 1. Assume that $\Omega = [m] \times [n]$, and that the initial guess (u_1, v_1) satisfies $\alpha_1, \beta_1 > 0$. Then the sequence of estimates (u_t, v_t) generated by R2RILS converges to (u, v) linearly with a contraction factor smaller than $\sqrt{1 - \frac{1}{\sqrt{2}}} \approx 0.54$. Specifically,

$$\left\| \begin{pmatrix} u_{t+1} \\ v_{t+1} \end{pmatrix} - \begin{pmatrix} u \\ v \end{pmatrix} \right\| = R(\epsilon_t, \delta_t) \left\| \begin{pmatrix} u_t \\ v_t \end{pmatrix} - \begin{pmatrix} u \\ v \end{pmatrix} \right\| \quad (14)$$

where

$$R(\epsilon_t, \delta_t) = \left[\frac{2 - r(\epsilon_t) - r(\delta_t)}{2 - \sqrt{1 - \epsilon_t^2} - \sqrt{1 - \delta_t^2}} \right]^{\frac{1}{2}} \leq \sqrt{1 - \frac{1}{\sqrt{2}}} \max\{\epsilon_t, \delta_t\},$$

and the function $r(\epsilon)$ was defined in Eq. (13) above.

Theorem 2. As $\epsilon_t, \delta_t \rightarrow 0$, the convergence is quadratic, with an asymptotic contraction factor of $\sqrt{\epsilon_t^4 - \epsilon_t^2 \delta_t^2 + \delta_t^4} \leq \sqrt{2} \max\{\epsilon_t^2, \delta_t^2\}$.

Remark 1. In the fully observed rank-1 case, it follows from the proof of Theorem 1 and can also be observed empirically that if the initial guess (u_1, v_1) is misaligned with the singular vectors (u, v) , namely $\alpha_1 \cdot \beta_1 < 0$, then R2RILS fails to converge. However, this has little practical significance, since if only some entries are observed and/or the rank is higher then with enough observed entries, empirically R2RILS converges to the exact low rank matrix.

Next, we present two remarks that theoretically motivate the choice of the minimal norm solution and the averaging step of R2RILS, both in the fully observed rank-1 case.

Remark 2. Consider a variant of R2RILS, where step II is replaced by

$$u_{t+1} = \text{ColNorm}(u_t + w_u \cdot \text{ColNorm}(\tilde{u}_t)), \quad v_{t+1} = \text{ColNorm}(v_t + w_v \cdot \text{ColNorm}(\tilde{v}_t)), \quad (15)$$

with weights $w_u, w_v \in \mathbb{R}$ that possibly depend on t . In the case $\Omega = [m] \times [n]$ and $\alpha_1, \beta_1 > 0$, it is possible to converge to the exact rank-1 matrix X_0 after a single iteration, by setting

$$w_u = (u_t^\top \text{ColNorm}(\tilde{u}_t))^{-1}, \quad w_v = (v_t^\top \text{ColNorm}(\tilde{v}_t))^{-1}. \quad (16)$$

Note that as $\epsilon_t, \delta_t \rightarrow 0$, namely as the current estimate becomes closer to (u, v) , then the optimal weights satisfy $w_u, w_v \rightarrow 1$, resulting in the original R2RILS. In other words, the averaging step of R2RILS is asymptotically optimal in the fully observed rank-1 case.

Remark 3. Assume $\Omega = [m] \times [n]$ and let $X = \sigma uv^\top$. By the proof of Lemma 2, in this case, the kernel of the linear map (9) is rank one, spanned by $(u_t, -v_t)$. Consider a variant where in step I, instead of the minimal norm solution $(\tilde{u}_t, \tilde{v}_t)$, it takes a solution of the form

$$\begin{pmatrix} \hat{u}_t \\ \hat{v}_t \end{pmatrix} = \begin{pmatrix} \tilde{u}_t \\ \tilde{v}_t \end{pmatrix} + \lambda_t \begin{pmatrix} u_t \\ -v_t \end{pmatrix}$$

where the scalar λ_t may in general depend on u_t, v_t and on t . Assume that (u_t, v_t) are aligned with (u, v) , namely $\alpha_t, \beta_t > 0$. Then, the only choice that leads to quadratic convergence of the column or row space as $\epsilon_t \rightarrow 0$ or $\delta_t \rightarrow 0$ is the minimal norm solution, namely $\lambda_t = 0$.

Finally, the following theorem shows that in the presence of additive Gaussian noise, the estimates (u_t, v_t) of R2RILS are close to the true vectors (u, v) up to an error term linear in the noise level. A similar result, with different constants, also holds for sub-Gaussian noise.

Theorem 3. *Let $\Omega = [m] \times [n]$, and assume w.l.o.g. that $\rho \equiv \sqrt{\frac{m}{n}} \leq 1$. Let $X = \sigma uv^\top + Z$ where $\sigma > 0$, $\|u\| = \|v\| = 1$ and all entries $Z_{i,j}$ are i.i.d. Gaussian with mean 0 and variance η_0^2 . Let $\delta \in (0, \frac{1}{4}]$, and assume the initial guess of R2RILS, (u_1, v_1) , satisfies $\alpha_1, \beta_1 \geq \delta$. Denote the normalized noise level $\eta \equiv \eta_0 \sqrt{n}$, and the constants $R \equiv \sqrt{1 - \frac{1}{\sqrt{2}}} \simeq 0.54$, $C \equiv \frac{50}{1-R}$. If*

$$\frac{\eta}{\sigma} \leq \frac{\sqrt{2}}{C} \cdot \delta, \quad (17)$$

then with probability at least $1 - e^{-\frac{n}{2}}$, for all $t \geq 2$,

$$\left\| \begin{pmatrix} u_t \\ v_t \end{pmatrix} - \begin{pmatrix} u \\ v \end{pmatrix} \right\| \leq \sqrt{3}R^{t-2} + 4C(1 - R^{t-2}) \frac{\eta}{\sigma}. \quad (18)$$

Hence, after $\log(\eta/\sigma)$ iterations, the error is $O(\eta/\sigma)$.

We first present the proof of Theorem 2 assuming Theorem 1 holds, and then present the proof of the latter. The proof of Theorem 3 appears in Appendix A.

Proof of Theorem 2. Since $h(\epsilon) = 1 + \epsilon^2 - 2\epsilon^4 + 2\epsilon^6 + \mathcal{O}(\epsilon^8)$, it follows that $r(\epsilon) = 1 - \frac{1}{2}\epsilon^6 + \mathcal{O}(\epsilon^8)$. Substituting these Taylor expansions into $R(\epsilon_t, \delta_t)$ gives

$$R(\epsilon_t, \delta_t) = \left[\frac{\epsilon_t^6 + \delta_t^6 + \mathcal{O}(\epsilon_t^8) + \mathcal{O}(\delta_t^8)}{\epsilon_t^2 + \delta_t^2 + \mathcal{O}(\epsilon_t^4) + \mathcal{O}(\delta_t^4)} \right]^{\frac{1}{2}} = \sqrt{\epsilon_t^4 - \epsilon_t^2 \delta_t^2 + \delta_t^4} \cdot (1 + o(1)).$$

□

To prove Theorem 1, we use the following lemma which provides a closed form expression to the minimal norm solution of Eq. (5), in the rank-1 case where all entries of the matrix have been observed. The proof of this auxiliary lemma appears in Appendix B.

Lemma 3. *Assume that $\Omega = [m] \times [n]$. Given non-zero vectors $(u_t, v_t) \in \mathbb{R}^m \times \mathbb{R}^n$ and an observed matrix X , the minimal norm solution to the least squares problem (5) is*

$$\tilde{u} = \frac{1}{\|v_t\|^2} \left(Xv_t - \frac{u_t^\top Xv_t}{N_t} u_t \right), \quad \tilde{v} = \frac{1}{\|u_t\|^2} \left(X^\top u_t - \frac{u_t^\top Xv_t}{N_t} v_t \right). \quad (19)$$

where $N_t = \|u_t\|^2 + \|v_t\|^2$. If the matrix X is rank-one, $X = \sigma uv^\top$ with $\sigma > 0$, and all vectors are normalized, $\|u\| = \|v\| = \|u_t\| = \|v_t\| = 1$, Eq. (19) simplifies to

$$\tilde{u} = \left(u - \frac{1}{2}\alpha_t u_t \right) \beta_t \sigma, \quad \tilde{v} = \left(v - \frac{1}{2}\beta_t v_t \right) \alpha_t \sigma \quad (20)$$

where $\alpha_t = u^\top u_t$ and $\beta_t = v^\top v_t$.

Proof of Theorem 1. It follows from Lemma 3, that the result of step I of R2RILS is given by Eq. (20). The normalized result is thus

$$\text{ColNorm}(\tilde{u}_t) = \frac{u - \frac{1}{2}\alpha_t u_t}{\tilde{\alpha}_t} \text{sign}(\beta_t), \quad \text{ColNorm}(\tilde{v}_t) = \frac{v - \frac{1}{2}\beta_t v_t}{\tilde{\beta}_t} \text{sign}(\alpha_t), \quad (21)$$

where $\tilde{\alpha}_t = \sqrt{1 - \frac{3\alpha_t^2}{4}}$ and $\tilde{\beta}_t = \sqrt{1 - \frac{3\beta_t^2}{4}}$. Assume for now that $\alpha_t, \beta_t > 0$. Later we will prove that $\alpha_1, \beta_1 > 0$ indeed implies $\alpha_t, \beta_t > 0$ for all $t \geq 1$. Then the next estimate is

$$u_{t+1} = \text{ColNorm}(u_t + \text{ColNorm}(\tilde{u}_t)) = \frac{u + (\tilde{\alpha}_t - \frac{1}{2}\alpha_t)u_t}{\sqrt{2 - \frac{3}{2}\alpha_t^2 + \alpha_t\tilde{\alpha}_t}}$$

with a similar expression for v_{t+1} . Their projections on the true vectors are

$$\alpha_{t+1} = u^\top u_{t+1} = \frac{1 + (\tilde{\alpha}_t - \frac{1}{2}\alpha_t)\alpha_t}{\sqrt{2 - \frac{3}{2}\alpha_t^2 + \alpha_t\tilde{\alpha}_t}}, \quad \beta_{t+1} = v^\top v_{t+1} = \frac{1 + (\tilde{\beta}_t - \frac{1}{2}\beta_t)\beta_t}{\sqrt{2 - \frac{3}{2}\beta_t^2 + \beta_t\tilde{\beta}_t}}. \quad (22)$$

The norm of the next estimate error is thus

$$E_{t+1} = \left\| \begin{pmatrix} u_{t+1} \\ v_{t+1} \end{pmatrix} - \begin{pmatrix} u \\ v \end{pmatrix} \right\| = \sqrt{2(2 - \alpha_{t+1} - \beta_{t+1})}.$$

Similarly, $E_t = \sqrt{2(2 - \alpha_t - \beta_t)}$. Finally we plug $\epsilon_t = \sqrt{1 - \alpha_t^2}$ and $\delta_t = \sqrt{1 - \beta_t^2}$. With $h(\epsilon_t)$ and $r(\epsilon_t)$ as defined in (13), $(\tilde{\alpha}_t - \frac{\alpha_t}{2})\alpha_t = \epsilon_t^2 + h(\epsilon_t)$ and $-\frac{3}{2}\alpha_t^2 + \alpha_t\tilde{\alpha}_t = 2(3\epsilon_t^2 + h(\epsilon_t))$, implying $\alpha_{t+1} = r(\epsilon_t)$ and $\beta_{t+1} = r(\delta_t)$. Thus $\frac{E_{t+1}}{E_t} = R(\epsilon_t, \delta_t)$.

To conclude the proof, we prove by induction that $\alpha_t, \beta_t > 0$ for all $t \geq 1$. At $t = 1$, the condition is one the assumptions of the theorem. Next, assuming $\alpha_t, \beta_t > 0$ yields Eq. (22). Since $\tilde{\alpha}_t - \alpha_t/2 \geq 0$ for any $\alpha_t \in [0, 1]$ then $\alpha_{t+1} > 0$. A similar proof holds for β_{t+1} . \square

Proof of Remark 2. Note that, following Eqs. (21), $w_u = \frac{2\tilde{\alpha}_t}{\alpha_t}$ and $w_v = \frac{2\tilde{\beta}_t}{\beta_t}$. Hence, the next estimate of the modified algorithm (15) is

$$u_{t+1} = \text{ColNorm}\left(u_t + w_u \text{ColNorm}\left(\left(u - \frac{\alpha_t u_t}{2}\right) \beta_t \sigma\right)\right) = \text{ColNorm}\left(u_t + \frac{\tilde{\alpha}_t}{\alpha_t} \frac{2u - \alpha_t u_t}{\tilde{\alpha}_t}\right) = u$$

and similarly $v_{t+1} = v$. Since $\alpha_t = \sqrt{1 - \epsilon_t^2} \rightarrow 1$ as $\epsilon_t \rightarrow 0$ and $w_u = \frac{2}{\alpha_t} \sqrt{1 - \frac{3\alpha_t^2}{4}} \rightarrow 1$ as $\alpha_t \rightarrow 1$, and similarly $w_v \rightarrow 1$ as $\delta_t \rightarrow 0$, the second part of the remark follows. \square

Proof of Remark 3. We focus on the column space part. The proof for the row space part is similar. The minimal norm solution \tilde{u}_t is given by (20). Hence, $\text{ColNorm}(\tilde{u}_t)$ cancels the factor $\beta_t \sigma$, decoupling it from the row estimate v_t and the singular value of X . In contrast, the column space part of the next estimate of the non-minimal norm solution (3) is

$$\hat{u}_{t+1} = \text{ColNorm}\left(u_t + \text{ColNorm}(\tilde{u}_t + \lambda_t u_t)\right) = \frac{\beta_t' u + (\gamma - \frac{1}{2}\alpha_t \beta_t' + \lambda_t) u_t}{\sqrt{\tilde{\alpha}_t^2 \beta_t'^2 + (\alpha_t \beta_t' + \gamma + \lambda_t)(\gamma + \lambda_t)}}$$

where $\beta'_t = \beta_t \sigma$, $\gamma = \sqrt{\tilde{\alpha}_t^2 \beta_t'^2 + \lambda_t \alpha_t \beta_t' + \lambda_t^2}$ and $\tilde{\alpha}_t = \sqrt{1 - \frac{3\alpha_t^2}{4}}$. Therefore,

$$\begin{aligned} \hat{\alpha}_{t+1} &= u^\top \hat{u}_{t+1} = \frac{\beta'_t + (\gamma - \frac{1}{2}\alpha_t \beta_t' + \lambda_t) \alpha_t}{\sqrt{\tilde{\alpha}_t^2 \beta_t'^2 + (\alpha_t \beta_t' + \gamma + \lambda_t)(\gamma + \lambda_t)}} \\ &= 1 - \frac{4\lambda_t^2}{(\beta'_t + 2\lambda)^2} (1 - \alpha_t) - \frac{2\beta'_t \lambda_t (4\beta_t'^2 - \beta_t' \lambda_t + 4\lambda_t^2)}{(\beta'_t + 2\lambda)^4} (1 - \alpha_t)^2 + \mathcal{O}((1 - \alpha_t)^3). \end{aligned}$$

It is easy to verify that $\hat{\alpha}_{t+1} = 1 + \mathcal{O}((1 - \alpha_t)^3)$ if and only if $\lambda_t = 0$. In fact, for any $\lambda_t \neq 0$, $\hat{\alpha}_{t+1} = 1 + \Theta(1 - \alpha_t)$. Indeed, $\hat{\alpha}_{t+1} = 1 + \mathcal{O}((1 - \alpha_t)^3)$ is a necessary and sufficient condition for quadratic convergence of the column space part, $\frac{\|\hat{u}_{t+1} - u\|}{\|u_t - u\|} = \mathcal{O}(\epsilon_t^2)$, since $\|\hat{u}_{t+1} - u\| = \sqrt{2(1 - \hat{\alpha}_{t+1})}$, $\|u_t - u\| = \sqrt{2(1 - \alpha_t)}$ and $\epsilon_t^2 = 1 - \alpha_t^2 = 2(1 - \alpha_t) + \mathcal{O}((1 - \alpha_t)^2)$. \square

A Proof of Theorem 3

First, we present two auxiliary lemmas regarding R2RILS in the presence of noise.

Lemma 4. *Under the conditions of Theorem 3, with probability at least $1 - e^{-\frac{n}{2}}$,*

$$\alpha_t, \beta_t \geq \frac{1}{4}, \quad \forall t \geq 2. \quad (23)$$

Lemma 5. *Denote by (u_{t+1}, v_{t+1}) and $(u_{t+1}^{(0)}, v_{t+1}^{(0)})$ the next estimate of R2RILS in the presence and in the absence of noise, starting from (u_t, v_t) . Let $\delta \in (0, \frac{1}{4}]$ and assume (u_t, v_t) satisfies $\alpha_t, \beta_t \geq \delta$. Then under the conditions of Theorem 3, w.p. at least $1 - e^{-\frac{n}{2}}$,*

$$\|u_{t+1} - u_{t+1}^{(0)}\| \leq \frac{50}{\sqrt{2}\delta} \frac{\eta}{\sigma} \quad \text{and} \quad \|v_{t+1} - v_{t+1}^{(0)}\| \leq \frac{50}{\sqrt{2}\delta} \frac{\eta}{\sigma}. \quad (24)$$

Proof of Theorem 3. Denote by E_t the ℓ_2 estimation error of R2RILS at iteration t ,

$$E_t = \left\| \begin{pmatrix} u_t \\ v_t \end{pmatrix} - \begin{pmatrix} u \\ v \end{pmatrix} \right\| = \sqrt{2(1 - \alpha_t) + 2(1 - \beta_t)}$$

Since by Lemma 4 $\alpha_2, \beta_2 \geq \frac{1}{4}$, then $E_2 \leq \sqrt{3}$. Let $u_{t+1}, v_{t+1}, u_{t+1}^{(0)}$ and $v_{t+1}^{(0)}$ be defined as in Lemma 5. Combining Lemma 4 and Theorem 1 gives that for the noiseless update

$$\left\| \begin{pmatrix} u_{t+1}^{(0)} \\ v_{t+1}^{(0)} \end{pmatrix} - \begin{pmatrix} u \\ v \end{pmatrix} \right\| \leq R \left\| \begin{pmatrix} u_t \\ v_t \end{pmatrix} - \begin{pmatrix} u \\ v \end{pmatrix} \right\| = RE_t. \quad (25)$$

Combining Lemma 4 and Lemma 5 with $\delta = \frac{1}{4}$ gives that with probability at least $1 - e^{-\frac{n}{2}}$

$$\left\| \begin{pmatrix} u_{t+1} \\ v_{t+1} \end{pmatrix} - \begin{pmatrix} u_{t+1}^{(0)} \\ v_{t+1}^{(0)} \end{pmatrix} \right\| \leq 200 \frac{\eta}{\sigma} = 4C(1 - R) \frac{\eta}{\sigma}. \quad (26)$$

Combining Eqs. (25), (26) and the triangle inequality gives that $E_{t+1} \leq RE_t + 4C(1 - R) \frac{\eta}{\sigma}$. Iteratively applying this recurrence relation, and the bound $E_2 \leq \sqrt{3}$, yields Eq. (18). \square

Proof of Lemma 4. In the absence of noise, by Theorem 1, $\alpha_t, \beta_t \geq \frac{1}{4}$ for all $t \geq 2$ as each iteration of R2RILS brings the estimate (u_t, v_t) closer to the singular vectors (u, v) . Eq. (23) holds also in the presence of low noise since the improvement in the estimate is larger than the effect of the noise. We prove this by induction. Since by assumption $\alpha_1, \beta_1 \geq \delta$ and $\delta \leq \frac{1}{4}$, it suffices to show that if $\alpha_t, \beta_t \geq \delta$ then $\alpha_{t+1}, \beta_{t+1} \geq 1/4$. From Eq. (22), for any $t \geq 1$, the minimal value of $\alpha_{t+1}^{(0)} = u_{t+1}^{(0)\top} u$ is $\frac{1}{\sqrt{2}}$, and thus $\|u_{t+1}^{(0)} - u\| = \sqrt{2(1 - \alpha_{t+1}^{(0)})} \leq R\sqrt{2}$. Combining Lemma 5 and assumption (17) gives that with probability at least $1 - e^{-\frac{\eta}{2}}$, $\|u_{t+1} - u_{t+1}^{(0)}\| \leq \frac{50}{\sqrt{2}\delta} \frac{\eta}{\sigma} \leq \frac{50}{C} = 1 - R$. Hence, by the triangle inequality,

$$\sqrt{2(1 - \alpha_{t+1})} = \|u_{t+1} - u\| \leq \|u_{t+1} - u_{t+1}^{(0)}\| + \|u_{t+1}^{(0)} - u\| \leq 1 - R + R\sqrt{2},$$

which implies $\alpha_{t+1} > \frac{1}{4}$. The proof for β_{t+1} is similar. \square

Finally, to prove Lemma 5, we use the following lemma on the largest singular value $\sigma_1(\bar{Z})$ of a Gaussian random matrix \bar{Z} , see [Davidson and Szarek, 2001, Theorem 2.13].

Lemma 6. *Let $m, n \in \mathbb{N}$ be such that $m \leq n$, and denote $\rho \equiv \sqrt{\frac{m}{n}} \leq 1$. Let $\bar{Z} \in \mathbb{R}^{m \times n}$ be a matrix whose entries $\bar{Z}_{i,j}$ are all i.i.d. $\mathcal{N}(0, 1/n)$. Then for any $s \geq 0$*

$$\mathbb{P}[\sigma_1(\bar{Z}) \leq 1 + \rho + s] \geq 1 - e^{-\frac{ns^2}{2}}. \quad (27)$$

Proof of Lemma 5. We prove the bound on u_{t+1} . The proof for v_{t+1} is similar. Given (u_t, v_t) , at iteration $t + 1$, R2RILS calculates three quantities: the minimal norm solution \tilde{u}_t to (5); its normalized version $\bar{u}_t \equiv \frac{\tilde{u}_t}{\|\tilde{u}_t\|}$; and the next estimate, $u_{t+1} = \frac{u_t + \bar{u}_t}{\|u_t + \bar{u}_t\|}$. The proof is divided into three steps, where we show that the ℓ_2 error of \tilde{u}_t , \bar{u}_t and u_{t+1} from their noiseless counterparts, denoted $\tilde{u}_t^{(0)}$, $\bar{u}_t^{(0)}$ and $u_{t+1}^{(0)}$ respectively, is bounded by terms linear in η .

Let us begin with the first step, in which we show that $\|\tilde{u}_t - \tilde{u}_t^{(0)}\| \lesssim \eta$. Plugging $X = \sigma u v^\top + Z$ into Eq. (19), the column space part of the minimal-norm solution of (5) is

$$\tilde{u}_t = \beta'_t u + Z v_t - \frac{\alpha_t \beta'_t + u_t^\top Z v_t}{2} u_t = \tilde{u}_t^{(0)} + \eta \left(I - \frac{1}{2} u_t u_t^\top \right) \bar{z}_{v,t}, \quad (28)$$

where $\beta'_t = \beta_t \sigma$, $\bar{z}_{v,t} = \bar{Z} v_t$ and $\tilde{u}_t^{(0)} = \beta'_t (u - \frac{\alpha_t}{2} u_t)$. For future use, note that

$$u_t^\top \tilde{u}_t^{(0)} = \frac{\alpha_t \beta'_t}{2} \quad \text{and} \quad \|\tilde{u}_t^{(0)}\| = \tilde{\alpha}_t \beta'_t \geq \frac{\beta'_t}{2} \quad (29)$$

where $\tilde{\alpha}_t = \sqrt{1 - \frac{3\alpha_t^2}{4}}$. Next, let $\zeta_{t,1} \equiv \bar{z}_{v,t}^\top u$ and $\zeta_{t,2} \equiv \bar{z}_{v,t}^\top u_t$. Since $\|u\| = \|u_t\| = \|v_t\| = 1$,

$$|\zeta_{t,1}|, |\zeta_{t,2}|, \|\bar{z}_{v,t}\| \leq \sigma_1(\bar{Z}). \quad (30)$$

By Lemma 6, with probability at least $1 - e^{-\frac{\eta}{2}}$, $\sigma_1(\bar{Z}) \leq 2 + \rho \leq 3$. From now on, we assume this event holds.

To bound $\|\tilde{u}_t - \tilde{u}_t^{(0)}\|$, it is convenient to decompose \tilde{u}_t , given by Eq. (28), into its component in the direction $\tilde{u}_t^{(0)}$ and an orthogonal component $\eta \tilde{w}$ with $\tilde{u}_t^{(0)} \perp \tilde{w}$:

$$\tilde{u}_t = (1 + \eta \tilde{r}) \tilde{u}_t^{(0)} + \eta \tilde{w} \quad (31)$$

where, by Eq. (29),

$$\tilde{r} = \bar{z}_{v,t}^\top \left(I - \frac{1}{2} u_t u_t^\top \right) \frac{\tilde{u}_t^{(0)}}{\left\| \tilde{u}_t^{(0)} \right\|^2} = \frac{1}{\tilde{\alpha}_t^2 \beta_t'} \left(\zeta_{t,1} - \frac{3}{4} \alpha_t \zeta_{t,2} \right) \quad (32)$$

and

$$\tilde{w} = \left(I - \frac{1}{2} u_t u_t^\top \right) \bar{z}_{v,t} - \tilde{r} \tilde{u}_t^{(0)} = \bar{z}_{v,t} - \frac{1}{2} \zeta_{t,2} u_t - \tilde{r} \tilde{u}_t^{(0)}.$$

For future use, and to conclude the first step of the proof, we now bound $|\tilde{r}|$ and $\|\tilde{w}\|$. Denote $D_1 \equiv \frac{1}{\delta\sigma}$. Combining Eq. (29), (30), $\sigma_1(\bar{Z}) \leq 3$ and the assumption $\alpha_t, \beta_t \geq \delta > 0$ gives

$$|\tilde{r}| \leq \frac{1 + \frac{3}{4} \alpha_t}{\tilde{\alpha}_t^2 \beta_t'} \sigma_1(\bar{Z}) \leq 21 D_1. \quad (33)$$

Combining Eqs. (29), (32), (30) and $\sigma_1(\bar{Z}) \leq 3$ and some algebraic manipulations yield

$$\|\tilde{w}\|^2 = \|\bar{z}_{v,t}\|^2 - \frac{(4\zeta_{t,1} - 3\alpha_t \zeta_{t,2})^2}{16\tilde{\alpha}_t^2} - \frac{3}{4} \zeta_{t,2}^2 \leq \|\bar{z}_{v,t}\|^2 \leq \sigma_1(\bar{Z})^2 \leq 9. \quad (34)$$

Since the bound on $\|\tilde{w}\|$ is independent of η , (31) concludes the first step of the proof.

Next, we bound $\left\| \bar{u}_t - \bar{u}_t^{(0)} \right\|$. By (31), $\|\bar{u}_t\|^2 = (1 + \tilde{r}\eta)^2 \left\| \tilde{u}_t^{(0)} \right\|^2 + \eta^2 \|\tilde{w}\|^2$. Thus

$$\bar{u}_t = \frac{(1 + \tilde{r}\eta) \tilde{u}_t^{(0)} + \eta \tilde{w}}{\sqrt{(1 + \tilde{r}\eta)^2 \left\| \tilde{u}_t^{(0)} \right\|^2 + \eta^2 \|\tilde{w}\|^2}} = \frac{\bar{u}_t^{(0)}}{\sqrt{1 + \tilde{\gamma}^2 \tilde{\eta}^2}} + \frac{\tilde{\eta} \tilde{\gamma}}{\sqrt{1 + \tilde{\gamma}^2 \tilde{\eta}^2}} \cdot \frac{\tilde{w}}{\|\tilde{w}\|}$$

where $\tilde{\eta} = \frac{\eta}{|1 + \tilde{r}\eta|}$ and $\tilde{\gamma} = \frac{\|\tilde{w}\|}{\left\| \tilde{u}_t^{(0)} \right\|}$. Combining Eqs. (34) and (29) and $\beta_t \geq \delta$ gives that $\tilde{\gamma} \leq 6D_1$.

This, together with the triangle inequality, implies that

$$\left\| \bar{u}_t - \bar{u}_t^{(0)} \right\|^2 = \left\| \tilde{a}_t \bar{u}_t^{(0)} - \frac{\tilde{\eta} \tilde{\gamma}}{\sqrt{1 + \tilde{\gamma}^2 \tilde{\eta}^2}} \cdot \frac{\tilde{w}}{\|\tilde{w}\|} \right\|^2 \leq \left(\tilde{a}_t \left\| \bar{u}_t^{(0)} \right\| + \tilde{\eta} \tilde{\gamma} \right)^2 \leq (\tilde{a}_t + 6D_1 \tilde{\eta})^2 \quad (35)$$

where $\tilde{a}_t = 1 - \frac{1}{\sqrt{1 + \tilde{\gamma}^2 \tilde{\eta}^2}}$. Next, we bound \tilde{a}_t and $\tilde{\eta}$ in Eq. (35). By assumption (17), $D_1 \eta \leq \frac{1}{75}$.

Combining this with Eq. (33) yields $|\tilde{r}| \eta \leq \frac{1}{3}$, and thus

$$\tilde{\eta} \leq \frac{3}{2} \eta. \quad (36)$$

To bound \tilde{a}_t , we use $\forall x : 1 - \frac{1}{\sqrt{1+x^2}} \leq \frac{x^2}{2}$, which implies $\tilde{a}_t \leq \frac{1}{2} \tilde{\gamma}^2 \tilde{\eta}^2 \leq \frac{9}{8} \tilde{\gamma}^2 \eta^2$. Since $\tilde{\gamma} < 6D_1$,

$$\tilde{a}_t \leq 41 D_1^2 \eta^2. \quad (37)$$

Inserting Eqs. (36) and (37) into Eq. (35) and recalling that $D_1 \eta \leq \frac{1}{75}$ yields

$$\left\| \bar{u}_t - \bar{u}_t^{(0)} \right\|^2 \leq (41 D_1^2 \eta^2 + 9 D_1 \eta)^2 \leq (10 D_1)^2 \eta^2 = D_2^2 \eta^2,$$

where $D_2 \equiv 10D_1$. Since D_2 is independent of η , the second step follows.

We now prove the third and final step. To this end, we decompose $(u_t + \bar{u}_t)$ into its component in the direction $u_t + \bar{u}_t^{(0)}$ and an orthogonal component $\eta\bar{w}$ with $(u_t + \bar{u}_t^{(0)}) \perp \bar{w}$:

$$u_t + \bar{u}_t = (1 + \bar{r}\eta) \left(u_t + \bar{u}_t^{(0)} \right) + \eta\bar{w} \quad (38)$$

where $\bar{r} = (\bar{w}')^\top \frac{u_t + \bar{u}_t^{(0)}}{\|u_t + \bar{u}_t^{(0)}\|^2}$ and $\bar{w} = \bar{w}' - \bar{r} \left(u_t + \bar{u}_t^{(0)} \right)$. Next, we bound $|\bar{r}|$ and $\|\bar{w}\|$. Combining Eq. (29) and Lemma 4 gives that $\|u_t + \bar{u}_t^{(0)}\|^2 = \left\| u_t + \frac{u - \frac{1}{2}\alpha_t u_t}{\alpha_t} \right\|^2 = 2 + \frac{2\alpha_t}{\alpha_t} \geq 2$. Recall that $\|u_t\| = \|\bar{u}_t^{(0)}\| = 1$ and $\|\bar{w}'\| \leq D_2$. Hence,

$$|\bar{r}| \leq \frac{\|\bar{w}'\| \left(\|u_t\| + \|\bar{u}_t^{(0)}\| \right)}{\|u_t + \bar{u}_t^{(0)}\|^2} \leq D_2. \quad (39)$$

This, in turn, together with the triangle inequality, implies the second bound

$$\|\bar{w}\|^2 \leq \left(\|\bar{w}'\| + |\bar{r}| \|u_t + \bar{u}_t^{(0)}\| \right)^2 \leq \left(\|\bar{w}'\| + |\bar{r}| \left(\|u_t\| + \|\bar{u}_t^{(0)}\| \right) \right)^2 \leq 9D_2^2. \quad (40)$$

Following (38), $\|u_t + \bar{u}_t\|^2 = (1 + \bar{r}\eta)^2 \|u_t + \bar{u}_t^{(0)}\|^2 + \eta^2 \|\bar{w}\|^2$, so the next estimate is

$$u_{t+1} = \frac{(1 + \bar{r}\eta) \left(u_t + \bar{u}_t^{(0)} \right) + \eta\bar{w}}{\sqrt{(1 + \bar{r}\eta)^2 \|u_t + \bar{u}_t^{(0)}\|^2 + \eta^2 \|\bar{w}\|^2}} = \frac{u_{t+1}^{(0)}}{\sqrt{1 + \bar{\gamma}^2 \bar{\eta}^2}} + \frac{\bar{\eta}\bar{\gamma}}{\sqrt{1 + \bar{\gamma}^2 \bar{\eta}^2}} \cdot \frac{\bar{w}}{\|\bar{w}\|}$$

where $\bar{\eta} = \frac{\eta}{|1 + \bar{r}\eta|}$ and $\bar{\gamma} = \frac{\|\bar{w}\|}{\|u_t + \bar{u}_t^{(0)}\|}$. Combining $\frac{1}{\|u_t + \bar{u}_t^{(0)}\|} \leq \frac{1}{\sqrt{2}}$ and Eq. (40) gives that $\bar{\gamma}^2 \leq 5D_2^2$. This, together with the triangle inequality, implies that

$$\|u_{t+1} - u_{t+1}^{(0)}\|^2 = \left\| \bar{a}u_{t+1}^{(0)} - \frac{\bar{\eta}\bar{\gamma}}{\sqrt{1 + \bar{\gamma}^2 \bar{\eta}^2}} \cdot \frac{\bar{w}}{\|\bar{w}\|} \right\|^2 \leq \left(\bar{a} \|u_{t+1}^{(0)}\| + \bar{\eta}\bar{\gamma} \right)^2 \leq \left(\bar{a} + \sqrt{5}D_2\bar{\eta} \right)^2 \quad (41)$$

where $\bar{a} = 1 - \frac{1}{\sqrt{1 + \bar{\gamma}^2 \bar{\eta}^2}}$. To show that $\|u_{t+1} - u_{t+1}^{(0)}\|$ is bounded by a term linear in η , we bound the two quantities \bar{a} and $\bar{\eta}$ in Eq. (41). Recall that $D_2 = 10D_1$. Since $D_1\eta \leq \frac{1}{75}$, we have $D_2\eta \leq \frac{1}{7}$. Combining it with Eq. (39) yields $|\bar{r}|\eta \leq \frac{1}{7}$, which implies the first bound

$$\bar{\eta} \leq \frac{7}{6}\eta. \quad (42)$$

To bound \bar{a} , we again use $\forall x : 1 - \frac{1}{\sqrt{1+x^2}} \leq \frac{x^2}{2}$ which implies $\bar{a} \leq \frac{1}{2}\bar{\gamma}^2\bar{\eta}^2 \leq \frac{4}{5}\bar{\gamma}^2\eta^2$. Since $\bar{\gamma}^2 \leq 5D_2^2$, we obtain $\bar{a} \leq 4D_2^2\eta^2$. Combining this bound on \bar{a} with Eqs. (42), (41) and recalling that $D_2\eta \leq \frac{1}{7}$ and $D_2 = 10D_1$ yields

$$\|u_{t+1} - u_{t+1}^{(0)}\|^2 \leq \left(4D_2^2\eta^2 + \frac{7\sqrt{5}}{6}D_2\eta \right)^2 \leq (3.2 \cdot 10D_1\eta)^2 \leq \left(\frac{50}{\sqrt{2}\delta} \frac{\eta}{\sigma} \right)^2.$$

□

B Proof of Auxiliary Lemma 3

For simplicity, we denote $\bar{u} = u_t$, $\bar{v} = v_t$ and $\text{Vec}(X) = \text{Vec}_{[m] \times [n]}(X)$ for the vector with entries $X_{i,j}$ for $(i,j) \in [m] \times [n]$. Let \tilde{A} be the matrix corresponding to the linear operator

$$\tilde{A} \begin{pmatrix} a \\ b \end{pmatrix} = \text{Vec}(\bar{u}b^\top + a\bar{v}^\top)$$

Note that in the rank-1 case, the least squares problem of Eq. (5) can be rewritten as

$$\text{argmin}_{a \in \mathbb{R}^m, b \in \mathbb{R}^n} \|\tilde{A} \begin{pmatrix} a \\ b \end{pmatrix} - \text{Vec}(X)\|_F. \quad (43)$$

Next, denote $f_n(i) := \lceil \frac{i}{n} \rceil$ and $g_n(i) := i \bmod n$. Then, $[\text{Vec}(B)]_i = B_{f_n(i), g_n(i)}$. Hence

$$\tilde{A}_{ij} = \begin{cases} \bar{v}_{g_n(i)} \delta_{f_n(i), j}, & j \leq m, \\ \bar{u}_{f_n(i)} \delta_{g_n(i), j-m}, & j > m. \end{cases}$$

Finally, the pseudo-inverse of the matrix \tilde{A} in (43) is given by the following lemma:

Lemma 7. *The Moore-Penrose pseudoinverse of \tilde{A} , $\tilde{A}^\dagger \in \mathbb{R}^{(m+n) \times (m+n)}$, is given by*

$$\tilde{A}^\dagger_{ij} = \begin{cases} \frac{\bar{v}_{g_n(j)}}{\|\bar{v}\|^2} (\delta_{i, f_n(j)} - \frac{1}{N} \bar{u}_i \bar{u}_{f_n(j)}), & i \leq m, \\ \frac{\bar{u}_{f_n(j)}}{\|\bar{u}\|^2} (\delta_{i-m, g_n(j)} - \frac{1}{N} \bar{v}_{i-m} \bar{v}_{g_n(j)}), & i > m \end{cases} \quad (44)$$

where $N = \|\bar{u}\|^2 + \|\bar{v}\|^2$.

Proof. We need to show that (i) $\tilde{A}\tilde{A}^\dagger\tilde{A} = \tilde{A}$, (ii) $\tilde{A}^\dagger\tilde{A}\tilde{A}^\dagger = \tilde{A}^\dagger$, and that (iii) $\tilde{A}\tilde{A}^\dagger$ and (iv) $\tilde{A}^\dagger\tilde{A}$ are Hermitian. By relatively simple calculations, the entries of $\tilde{A}\tilde{A}^\dagger \in \mathbb{R}^{(mn) \times (mn)}$ are

$$\left(\tilde{A}\tilde{A}^\dagger\right)_{ij} = \delta_{f_n(i), f_n(j)} \delta_{g_n(i), g_n(j)} - \left(\delta_{f_n(i), f_n(j)} - \frac{\bar{u}_{f_n(i)} \bar{u}_{f_n(j)}}{\|\bar{u}\|^2}\right) \left(\delta_{g_n(i), g_n(j)} - \frac{\bar{v}_{g_n(i)} \bar{v}_{g_n(j)}}{\|\bar{v}\|^2}\right).$$

Similar calculations for $\tilde{A}^\dagger\tilde{A} \in \mathbb{R}^{(m+n) \times (m+n)}$ give

$$\left(\tilde{A}^\dagger\tilde{A}\right)_{ij} = \begin{cases} \delta_{i,j} - \frac{1}{N} \bar{u}_i \bar{u}_j, & i \leq m \text{ and } j \leq m, \\ \frac{1}{N} \bar{u}_i \bar{v}_{j-m}, & i \leq m \text{ and } j > m, \\ \frac{1}{N} \bar{v}_{i-m} \bar{u}_j, & i > m \text{ and } j \leq m, \\ \delta_{i,j} - \frac{1}{N} \bar{v}_{i-m} \bar{v}_{j-m}, & i > m \text{ and } j > m. \end{cases}$$

Since these two matrices are Hermitian, conditions (iii)-(iv) are fulfilled. It is now simple to verify that $\tilde{A}\tilde{A}^\dagger\tilde{A} = \tilde{A}$ and $\tilde{A}^\dagger\tilde{A}\tilde{A}^\dagger = \tilde{A}^\dagger$. Thus conditions (i)-(ii) are also fulfilled. \square

Proof of Lemma 3. Since problem (5) is equivalent to (43), its minimal norm solution is $\begin{pmatrix} \tilde{u} \\ \tilde{v} \end{pmatrix} = \tilde{A}^\dagger \text{Vec}(X)$, with \tilde{A}^\dagger given by (44). An explicit calculation yields (19). Eq. (20) follows by plugging $X = \sigma uv^\top$. \square

Acknowledgments

We would like to especially thank Yuval Kluger for pointing us at the direction of matrix completion and for inspiring conversations along the way. We thank Laura Balzano, Nicolas Boumal, Rachel Ward, Rong Ge, Eric Chi, Chen Greif and Haim Avron for interesting discussions. BN is incumbent of the William Petschek professorial chair of mathematics. BN was supported by NIH grant R01GM135928 and by Pazy foundation grant ID77-2018. Part of this work was done while BN was on sabbatical at the Institute for Advanced Study at Princeton. He gratefully acknowledges the support from the Charles Simonyi Endowment.

References

- Haim Avron, Satyen Kale, Shiva Prasad Kasiviswanathan, and Vikas Sindhwani. Efficient and practical stochastic subgradient descent for nuclear norm regularization. In *Proceedings of the 29th International Conference on Machine Learning*, pages 323–330, Madison, WI, USA, 2012. Omnipress.
- Laura Balzano, Robert Nowak, and Benjamin Recht. Online identification and tracking of subspaces from highly incomplete information. In *2010 48th Annual allerton conference on communication, control, and computing (Allerton)*, pages 704–711. IEEE, 2010.
- Jeffrey D Blanchard, Jared Tanner, and Ke Wei. CGIHT: conjugate gradient iterative hard thresholding for compressed sensing and matrix completion. *Information and Inference: A Journal of the IMA*, 4(4):289–327, 2015.
- Nicolas Boumal and P-A Absil. Low-rank matrix completion via preconditioned optimization on the grassmann manifold. *Linear Algebra and its Applications*, 475:200–239, 2015.
- Aeron M Buchanan and Andrew W Fitzgibbon. Damped newton algorithms for matrix factorization with missing data. In *Conference on Computer Vision and Pattern Recognition (CVPR)*, volume 2, pages 316–322. IEEE, 2005.
- Jian-Feng Cai, Emmanuel J Candès, and Zuowei Shen. A singular value thresholding algorithm for matrix completion. *SIAM Journal on Optimization*, 20(4):1956–1982, 2010.
- Emmanuel J Candès and Yaniv Plan. Matrix completion with noise. *Proceedings of the IEEE*, 98(6):925–936, 2010.
- Emmanuel J Candès and Benjamin Recht. Exact matrix completion via convex optimization. *Foundations of Computational mathematics*, 9(6):717, 2009.
- Emmanuel J Candès and Terence Tao. The power of convex relaxation: Near-optimal matrix completion. *IEEE Transactions on Information Theory*, 56(5):2053–2080, 2010.
- Yudong Chen, Srinadh Bhojanapalli, Sujay Sanghavi, and Rachel Ward. Completing any low-rank matrix, provably. *The Journal of Machine Learning Research*, 16(1):2999–3034, 2015.
- Yuxin Chen, Jianqing Fan, Cong Ma, and Yuling Yan. Inference and uncertainty quantification for noisy matrix completion. *Proceedings of the National Academy of Sciences*, 116(46):22931–22937, 2019.

- Eric C Chi and Tianxi Li. Matrix completion from a computational statistics perspective. *Wiley Interdisciplinary Reviews: Computational Statistics*, 11(5):e1469, 2019.
- Yuejie Chi, Yue M Lu, and Yuxin Chen. Nonconvex optimization meets low-rank matrix factorization: An overview. *IEEE Transactions on Signal Processing*, 67(20):5239–5269, 2019.
- Mark A Davenport and Justin Romberg. An overview of low-rank matrix recovery from incomplete observations. *IEEE Journal of Selected Topics in Signal Processing*, 10(4):608–622, 2016.
- Kenneth R Davidson and Stanislaw J Szarek. Local operator theory, random matrices and banach spaces. *Handbook of the geometry of Banach spaces*, 1(317-366):131, 2001.
- Maryam Fazel, Haitham Hindi, Stephen P Boyd, et al. A rank minimization heuristic with application to minimum order system approximation. *Proceedings of the American control conference*, 6:4734–4739, 2001.
- Massimo Fornasier, Holger Rauhut, and Rachel Ward. Low-rank matrix recovery via iteratively reweighted least squares minimization. *SIAM Journal on Optimization*, 21(4):1614–1640, 2011.
- Rong Ge, Jason D Lee, and Tengyu Ma. Matrix completion has no spurious local minimum. In *Advances in Neural Information Processing Systems*, pages 2973–2981, 2016.
- David Gross. Recovering low-rank matrices from few coefficients in any basis. *IEEE Transactions on Information Theory*, 57(3):1548–1566, 2011.
- Justin P Haldar and Diego Hernando. Rank-constrained solutions to linear matrix equations using powerfactorization. *IEEE Signal Processing Letters*, 16(7):584–587, 2009.
- Moritz Hardt. Understanding alternating minimization for matrix completion. In *2014 IEEE 55th Annual Symposium on Foundations of Computer Science*, pages 651–660. IEEE, 2014.
- Ken Hayami. Convergence of the conjugate gradient method on singular systems. *arXiv preprint arXiv:1809.00793*, 2018.
- Je Hyeong Hong and Andrew Fitzgibbon. Secrets of matrix factorization: Approximations, numerics, manifold optimization and random restarts. In *Proceedings of the IEEE International Conference on Computer Vision*, pages 4130–4138, 2015.
- Prateek Jain and Praneeth Netrapalli. Fast exact matrix completion with finite samples. In *Conference on Learning Theory*, pages 1007–1034, 2015.
- Prateek Jain, Praneeth Netrapalli, and Sujay Sanghavi. Low-rank matrix completion using alternating minimization. In *Proceedings of the forty-fifth annual ACM symposium on Theory of computing*, pages 665–674. ACM, 2013.
- Shuiwang Ji and Jieping Ye. An accelerated gradient method for trace norm minimization. In *Proceedings of the 26th annual international conference on machine learning*, pages 457–464. ACM, 2009.
- Raghunandan H Keshavan, Andrea Montanari, and Sewoong Oh. Matrix completion from a few entries. *IEEE transactions on Information Theory*, 56(6):2980–2998, 2010.

- Christian Kümmerle and Juliane Sigl. Harmonic mean iteratively reweighted least squares for low-rank matrix recovery. *The Journal of Machine Learning Research*, 19(1):1815–1863, 2018.
- Anastasios Kyrillidis and Volkan Cevher. Matrix recipes for hard thresholding methods. *Journal of mathematical imaging and vision*, 48(2):235–265, 2014.
- Shiqian Ma, Donald Goldfarb, and Lifeng Chen. Fixed point and Bregman iterative methods for matrix rank minimization. *Mathematical Programming*, 128(1-2):321–353, 2011.
- Goran Marjanovic and Victor Solo. On ℓ_q optimization and matrix completion. *IEEE Transactions on signal processing*, 60(11):5714–5724, 2012.
- Rahul Mazumder, Trevor Hastie, and Robert Tibshirani. Spectral regularization algorithms for learning large incomplete matrices. *Journal of machine learning research*, 11(Aug):2287–2322, 2010.
- Bamdev Mishra and Rodolphe Sepulchre. R3MC: A Riemannian three-factor algorithm for low-rank matrix completion. In *53rd IEEE Conference on Decision and Control*, pages 1137–1142. IEEE, 2014.
- Bamdev Mishra, Gilles Meyer, Silvère Bonnabel, and Rodolphe Sepulchre. Fixed-rank matrix factorizations and Riemannian low-rank optimization. *Computational Statistics*, 29(3-4):591–621, 2014.
- Thanh Ngo and Yousef Saad. Scaled gradients on grassmann manifolds for matrix completion. In *Advances in Neural Information Processing Systems*, pages 1412–1420, 2012.
- Takayuki Okatani and Koichiro Deguchi. On the wiberg algorithm for matrix factorization in the presence of missing components. *International Journal of Computer Vision*, 72(3):329–337, 2007.
- Takayuki Okatani, Takahiro Yoshida, and Koichiro Deguchi. Efficient algorithm for low-rank matrix factorization with missing components and performance comparison of latest algorithms. In *International Conference on Computer Vision*, pages 842–849. IEEE, 2011.
- Christopher C Paige and Michael A Saunders. LSQR: An algorithm for sparse linear equations and sparse least squares. *ACM Transactions on Mathematical Software (TOMS)*, 8(1):43–71, 1982.
- Daniel L Pimentel-Alarcón, Nigel Boston, and Robert D Nowak. A characterization of deterministic sampling patterns for low-rank matrix completion. *IEEE Journal of Selected Topics in Signal Processing*, 10(4):623–636, 2016.
- Benjamin Recht. A simpler approach to matrix completion. *Journal of Machine Learning Research*, 12(Dec):3413–3430, 2011.
- Benjamin Recht and Christopher Ré. Parallel stochastic gradient algorithms for large-scale matrix completion. *Mathematical Programming Computation*, 5(2):201–226, 2013.
- Jasson DM Rennie and Nathan Srebro. Fast maximum margin matrix factorization for collaborative prediction. In *Proceedings of the 22nd international conference on Machine learning*, pages 713–719. ACM, 2005.

- Amit Singer and Mihai Cucuringu. Uniqueness of low-rank matrix completion by rigidity theory. *SIAM Journal on Matrix Analysis and Applications*, 31(4):1621–1641, 2010.
- Ruoyu Sun and Zhi-Quan Luo. Guaranteed matrix completion via non-convex factorization. *IEEE Transactions on Information Theory*, 62(11):6535–6579, 2016.
- Jared Tanner and Ke Wei. Normalized iterative hard thresholding for matrix completion. *SIAM Journal on Scientific Computing*, 35(5):S104–S125, 2013.
- Jared Tanner and Ke Wei. Low rank matrix completion by alternating steepest descent methods. *Applied and Computational Harmonic Analysis*, 40(2):417–429, 2016.
- Kim-Chuan Toh and Sangwoon Yun. An accelerated proximal gradient algorithm for nuclear norm regularized linear least squares problems. *Pacific Journal of optimization*, 6(615-640):15, 2010.
- Bart Vandereycken. Low-rank matrix completion by Riemannian optimization. *SIAM Journal on Optimization*, 23(2):1214–1236, 2013.
- Ke Wei, Jian-Feng Cai, Tony F Chan, and Shingyu Leung. Guarantees of Riemannian optimization for low rank matrix recovery. *SIAM Journal on Matrix Analysis and Applications*, 37(3):1198–1222, 2016.
- Zaiwen Wen, Wotao Yin, and Yin Zhang. Solving a low-rank factorization model for matrix completion by a nonlinear successive over-relaxation algorithm. *Mathematical Programming Computation*, 4(4):333–361, 2012.
- T Wiberg. Computation of principal components when data are missing. In *Proc. Second Symp. Computational Statistics*, pages 229–236, 1976.